PHILOSOPHICAL TRANSACTIONS OF THE ROYAL SOCIETY B BIOLOGICAL SCIENCES

Modelling the interactions between ammonium and nitrate uptake in marine phytoplankton

Kevin J. Flynn, Michael J. R. Fasham and Charles R. Hipkin

Phil. Trans. R. Soc. Lond. B 1997 **352**, 1625-1645
doi: 10.1098/rstb.1997.0145

Modelling the interactions between ammonium and nitrate uptake in marine phytoplankton

KEVIN J. FLYNN[1], MICHAEL J. R. FASHAM[2] AND CHARLES R. HIPKIN[1]

[1]*Swansea Algal Research Unit, School of Biological Sciences, University of Wales Swansea, Singleton Park, Swansea SA2 8PP, UK* (k.j.flynn@swansea.ac.uk)
[2]*Southampton Oceanography Centre, Empress Dock, Southampton SO14 3ZH, UK*

CONTENTS

SUMMARY

An empirically based mathematical model is presented which can simulate the major features of the interactions between ammonium and nitrate transport and assimilation in phytoplankton. The model (ammonium–nitrate interaction model), which is configured to simulate a generic microalga rather than a specified species, is constructed on simplified biochemical bases. A major requirement for parametrization is that the N:C ratio of the algae must be known and that transport and internal pool sizes need to be expressed per unit of cell C. The model uses the size of an internal pool of an early organic product of N assimilation (glutamine) to regulate rapid responses in ammonium–nitrate interactions. The synthesis of enzymes for the reduction of nitrate through to ammonium is induced by the size of the internal nitrate pool and repressed by the size of the glutamine pool. The assimilation of intracellular ammonium (into glutamine) is considered to be a constitutive process subjected to regulation by the size of the glutamine pool. Longer term responses have been linked to the nutrient history of the cell using the N:C cell quota. N assimilation in darkness is made a function of the amount of surplus C present and thus only occurs at low values of N:C. The model can simulate both qualitative and quantitative temporal shifts in the ammonium–nitrate interaction, while inclusion of a derivation of the standard quota model enables a concurrent simulation of cell growth and changes in nutrient status.

1. INTRODUCTION

Nitrogen assimilation in eukaryotic algae is a resource-expensive process that is coupled closely with autotrophic and heterotrophic carbon metabolism (Turpin *et al.* 1988; Turpin 1991). Numerous studies over the last 40 years have demonstrated that it is highly regulated and subject to reversible biochemical modulation (e.g. rapid inhibition of nitrate uptake on supply of ammonium) as well as coarser, long-term control at the genetic level (e.g. induction and repression of enzymes and uptake systems (Solomonson & Barber 1990)). Even so, our understanding of these processes in most marine phytoplankton is confined to the phenomenological level and mechanisms for the fine control of enzyme systems are poorly understood. Nevertheless, there is compelling evidence that an early organic product of inorganic nitrogen assimilation plays a central role in short-term and long-term metabolic regulation of nitrate assimilation (Cullimore & Sims 1981*a*; Syrett 1981; Flynn 1991). It has been a major goal of marine phytoplankton ecology to translate such knowledge,

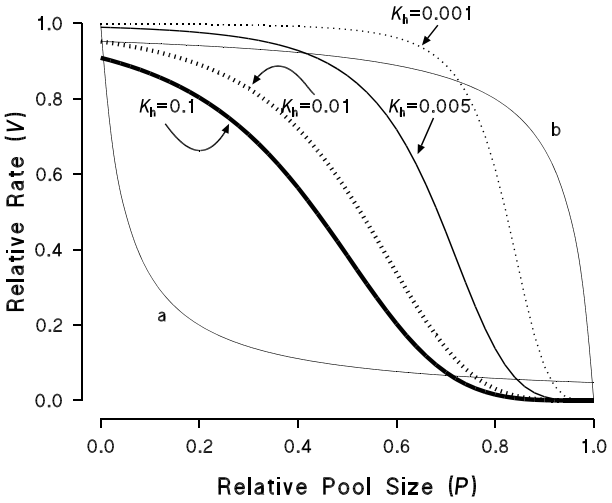

Figure 1. Plot showing the sigmoidal relationship between a rate process and the size of its regulatory pool according to the general equation $V = (1 - P)^4/((1 - P)^4 + Kh)$, where the relative pool size is $P = (\text{pool} \cdot \text{maximum pool}^{-1})$, Kh is a constant and V is the relative rate of the controlled process. Curves for different values of Kh are shown. For comparison, curves a and b are rectangular hyperbolic (Michaelis–Menten type) functions with equations $V = 1 - (P/(P + K))$ and $V = (1 - P)/(1 - P + K)$, respectively, with constant K set at 0.05.

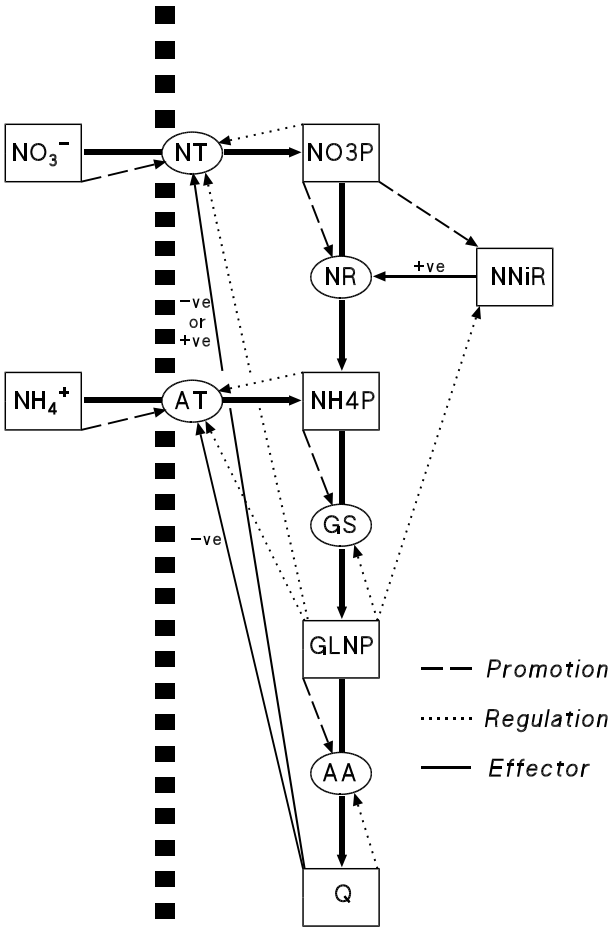

Figure 2. Overview of the model. NO3P, NH4P, GLNP and Q are internal pools of nitrate, ammonium, glutamine and other organic cellular N, respectively. NNiR is nitrate–nitrite reductase, and GS glutamine synthetase activities. NT and AT are nitrate and ammonium transporters, respectively, NR describes the process of nitrate reduction through to ammonium, and AA the synthesis of amino acids and all other nitrogenous compounds from GLN. 'Promotion', 'regulation' and 'effector' are used in general terms, with no specific biochemical meaning, indicating positive, negative or complex feedbacks, respectively.

derived from both laboratory and field-based experiments, into a practical understanding of the physiological ecology of phytoplankton nitrogen nutrition.

Some of the most striking ecophysiological interactions in algal nitrogen metabolism include those that arise from the antagonism between nitrate and ammonium assimilation (Conway 1977; Cresswell & Syrett 1979; Blasco & Conway 1982; Wheeler 1983; Glibert & McCarthy 1984; Lund 1987; Dortch 1990; Flynn 1991). In particular, changes in the degree of preference for ammonium over nitrate, especially in terms of the nutritional status of the cells (e.g. Dortch & Conway 1984; Syrett *et al.* 1986) have attracted considerable attention. With increasing concern over the implications of global warming, interest in these interactions has heightened since the proportion of phytoplankton growth supported by oxidized forms of inorganic nitrogen (primarily nitrate) indicates 'new' production (Dugdale & Goering 1967) which is coupled with the transfer of fixed carbon from surface waters to burial in sediments.

Progress requires the formulation of a mathematical model that will allow predictions about phytoplankton growth to be made in terms of the quantity of available nitrate and ammonium. An advantage in this approach is the simulation of transient interactions that occur in nature at very low nutrient concentrations (nM, e.g. Harrison *et al.* 1996) which are very difficult to reproduce in laboratory experiments.

The aim of this paper is to present a more complete mathematical model than has been previously formulated which is capable of simulating the transient responses of phytoplankton populations to the supply of nitrate and ammonium. This in turn must conform to the key elements in our knowledge of the physiology of nitrate-ammonium interactions, summarized in table 1.

2. THEORETICAL BASES AND MODEL DEVELOPMENT

(*a*) *Model construction*

The model was formulated on the PowerSim package (Bergen, Norway), which is based on the format of 'Forrester models' (the formulation and use of such models in biology is described by Haefner (1996)). PowerSim models contain levels (state variables or accumulators such as internal nutrient pool sizes and external nutrient concentration), constants, auxiliaries (products or sums of constants, levels, or other auxiliaries) and flows between levels (usually these are auxiliaries). The model could be con-

PHILOSOPHICAL TRANSACTIONS OF THE ROYAL SOCIETY B BIOLOGICAL SCIENCES

Table 1. *Summary of major aspects of the interaction between ammonium and nitrate use by phytoplankton*

aspect	example references
(i) above a threshold concentration of NH_4^+, NO_3^- use is inhibited	McCarthy *et al.* 1975; Maestrini *et al.* 1986; Quegumer *et al.* 1986; Dortch 1990
(ii) N replete cells using NH_4^+ cannot immediately use nitrate	Syrett & Hipkin 1973; Syrett 1981
(iii) cells using NO_3^- can immediately use NH_4^+ at high rates	Horrigan & McCarthy 1982; Dixon & Syrett 1988
(iv) NH_4^+ inhibition of NO_3^- uptake is not due to NH_4^+ *per se* but a product of its assimilation	Syrett & Morris 1963; Rigano *et al.* 1979
(v) NO_3^- and NH_4^+ do not share the same porter	Raven 1980; Syrett 1981; Syrett & Peplinska 1988
(vi) affinity of transporters do not appear to alter with N stress	Eppley *et al.* 1969*b*; Dortch 1990
(vii) ability to take up and assimilate NH_4^+ and NO_3^- develops with N stress under certain conditions	Syrett 1956*a*; Hipkin *et al.* 1983; Syrett *et al.* 1986; Syrett & Peplinska 1988
(viii) NH_4^+ grown cells may have a higher N:C ratio	Wood & Flynn 1995; Flynn *et al.* 1996
(ix) NO_3^- and free amino acids readily accumulate, but NH_4^+ accumulates to much lower concentrations within cells	Dortch 1982; Dortch *et al.* 1984
(x) NH_4^+ grown cells have higher free amino acid pools and higher glutamine and N stressed cells have small pools	Flynn 1990*a*,*b*; Wood & Flynn 1995
(xi) cells using NO_3^- must expend significant amounts of energy on reduction through to NH_4^+; this may have adverse affects on NO_3^- assimilation in the dark	Syrett 1956*b*; Losada 1980
(xii) despite (viii)–(xi), there may be little if any improvement in growth rates when using NH_4^+; any improvement appears at higher light	Thompson *et al.* 1989; Levasseur *et al.* 1993
(xiii) only N stressed cells (low N:C) can assimilate N in the dark and this assimilation stops at a lower N:C ratio for NO_3^- than for NH_4^+	Syrett 1956*b*; Cullen & Horrigan 1981; Paasche *et al.* 1984; Rainbault & Mingazzini 1987
(xiv) the enzymes of the NO_3^- assimilation pathway are inducible	Syrett 1981; Solomonson & Barber 1990
(xv) glutamine synthetase is constitutive but subject to post-transcriptional regulation	Miflin & Lee 1980; Cullimore & Sims 1981*a*
(xvi) internal NO_3^- may continue to be reduced *in vivo* after uptake has been inhibited following the uptake of NH_4^+	Cresswell & Syrett 1979

figured to operate on any package offering Runga–Kutta variable step integration of the 4th order.

Any biochemically based model of the interaction between ammonium and nitrate during transport and assimilation into microalgae will contain various feedback mechanisms. Such mechanisms are often simulated using simple Michaelis–Menten (rectangular hyperbolic, or RH) functions to describe links between concentrations and rates. However, the use of RH curves to regulate pool processes results in unreasonably rapid changes in rates with small changes in pool sizes and pools which are normally nearly empty or nearly full (for example, see figure 1 curves a and b). In reality these relationships may be better simulated using empirical sigmoidal curves in keeping with the likely allosteric nature of the enzyme processes.

The generic equations for these response curves are of the form

$$V = Vmax \cdot \frac{S^n}{S^n + Kh}$$

for an increasing rate (positive function) and

$$V = Vmax \cdot \frac{(1-S)^n}{(1-S)^n + Kh}$$

for a decreasing rate, where S is the relative pool size, given by

$$(\text{pool size}) \cdot (\text{maximum pool size})^{-1},$$

Vmax is the maximum rate, V the rate and Kh a constant.

If n = 1 these equations describe RH functions with Kh analogous to Km for enzyme reactions and to Ks for transport. The value of S which will allow 95% of Vmax in RH curves is 20 times the half saturation constant; in ignorance of other information Kh for RH curves may be set at 1–5% of the maximum pool size. We have used RH curves to control processes relating to substrate concentrations (i.e. transport, inhibition of transport from the size of the internal pool and enzymic reactions).

For sigmoidal (Hill) functions, n has been set at 4 and different values of Kh used in order to vary the shape of the curve (see figure 1 for regulatory or negative feedback curves). Sigmoidal equations with n = 4 have been used because this is the lowest value which gave a series of curves with sufficient (realistic) lag at high and low pool sizes. Sigmoidal curves have been used for all feedback processes.

The structure of the model is presented in simplified form in figure 2, with the form of the PowerSim model in figure 3. Parameter values, definitions and equations are given in tables 2 to 7; reference to equations in the text is by number thus: equation [table

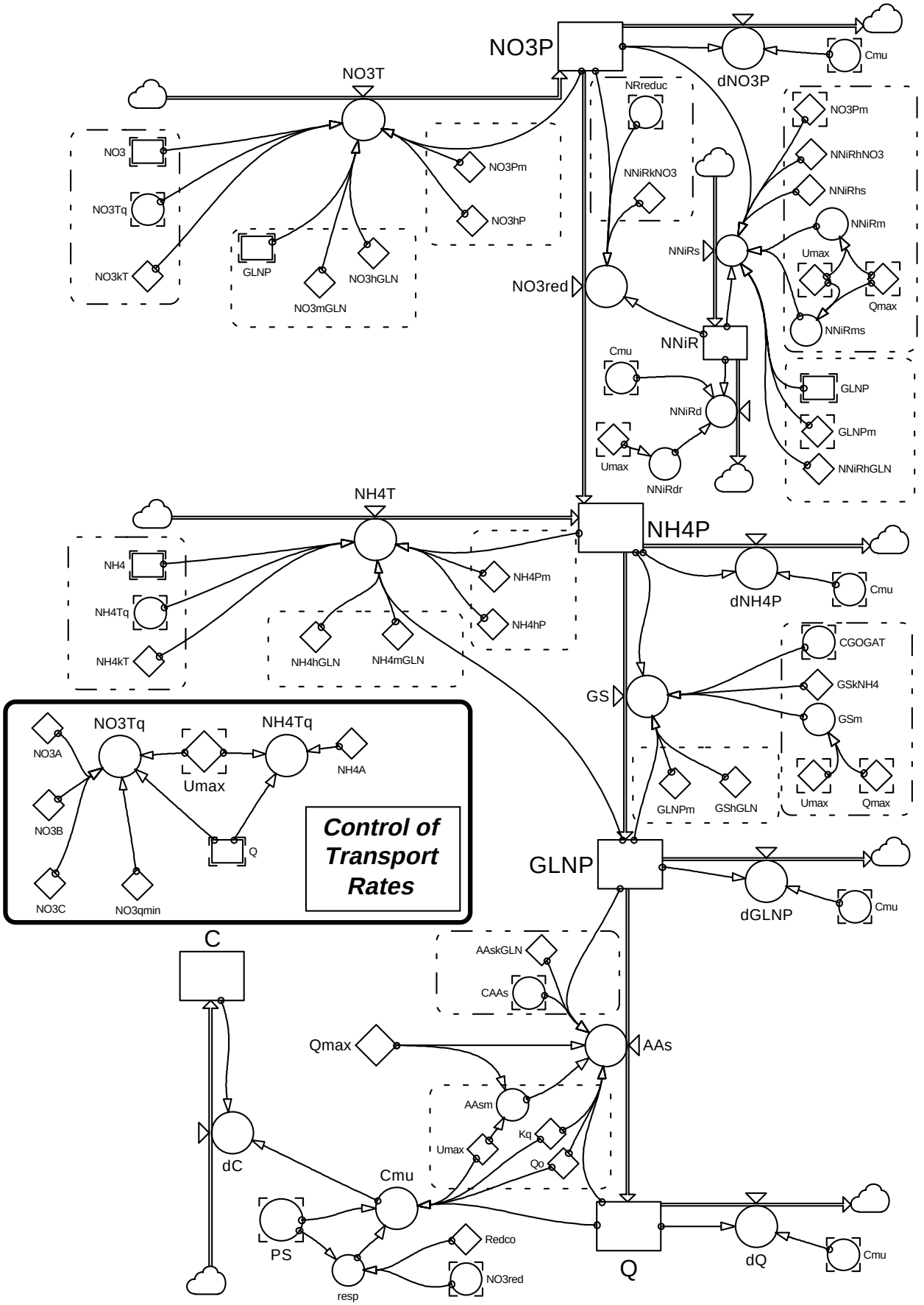

Figure 3. Structure of the PowerSim model, excluding the calculation of C for N assimilation in darkness and changes in external nutrient concentration. Boxes are levels (table 3), diamonds are constants (table 2), circles are auxiliaries (products of connected parameters), circles with pipes are flows and clouds represent sources or sinks. Where possible, symbols have been grouped togther to indicate common blocks within the model. Symbols within box corners are duplicate parameters which may appear several times elsewhere in the model.

no.x]. As far as possible the names of parameters follow a convention by which, 's' denotes synthesis, 'm' maximum, 'h' a Hill constant, 'k' a Michaelis–Menten (RH) constant, 'T' transport, 'P' pool, 'q' donates a function of Q (the N status of the cell), the first mentioned level is that being operated on and a second level the regulator. Hence, for example, $NO3hGLN$ is the Hill constant for the repression of nitrate transport by glutamine, $GLNPm$ is the maximum size of the glutamine pool, $NH4kT$ the Michaelis–Menten constant for ammonium transport and NH4Tq the maximum rate of ammonium transport at the current N status (value of Q).

As an overview (figures 2 and 3), nitrate and ammonium are transported into the cell, where they enter internal nutrient pools. Following reduction of internal nitrate to ammonium, the contents of the ammonium pool is used in the synthesis of the amino acid glutamine (GLN) and then to make other nitrogenous cellular materials (collectively termed Q, the nitrogen quota of the cell). The value of Q is then used to regulate the growth of the cell C. There are various levels of feedback between the internal pools, as indicated in figure 2, and explained below. Regulatory curves have been normalized to maximum pool sizes and to the maximum growth rate ($Umax$); although this complicates the equations it enables the use of different maximum pool sizes and growth rates without requiring modifications to the model.

External nutrient concentrations and phytoplankton biomass have units of the mass of N or C per unit volume. The size of internal nutrient pools, and the flows between them, are all described as mass ratios of N per unit of C. (In order to convert these ratios into molar concentrations for internal nutrient pools it is necessary to know the relationship between C and biovolume, say 0.2 g C ml^{-1} or 1 μg C = 5×10^{-9} l, and also to assume that the internal pool is not compartmentalized.) Because the level of internal nutrient pools are N:C ratios, these need to be corrected for changes in C with cell growth, thus

$$\frac{d}{dt}\left[\frac{N}{C}\right] = \frac{1}{C}\cdot\frac{dN}{dt} - \frac{N}{C^2}\cdot\frac{dC}{dt}$$
$$= \frac{1}{C}\cdot\frac{dN}{dt} - Cmu\cdot\frac{N}{C},$$

where the C-specific growth rate is given as

$$Cmu = \frac{1}{C}\cdot\frac{dC}{dt}$$

and N/C is the size of the pool in question.

The model is configured to simulate both light and dark processes. During darkness, although C growth is not allowed, N assimilation (and hence transport) can continue as long as there remains sufficient surplus C (i.e. Q remains low) to support it. The availability of C for N assimilation (defined as CGOGAT and CAAs for the synthesis of GLN and amino acids leading to Q, respectively) and of reductant for the conversion of nitrate to ammonium (NRreduc) are made inverse sigmoidal functions of Q (figure 4, equation 4.2–4.5). Assimilation of N in darkness depletes the surplus C and increases Q. The rate of reduction of nitrate through to ammonium is restricted to a proportion of that which occurs in the light when photo-generated reductant would be available. In this instance we have used a value of 60% (equation 4.3); Watanabe *et al.* (1982) suggest values between 41 and 100% of light rates may be attained in the dark. The respiratory cost in terms of C for the supply reductant for assimilation of nitrate through to ammonium has also been accounted for (see later). There is no general respiration term in the current form of this model.

(*b*) *Control of transport (figures 2, 3; equation 5.x in table 5)*

The maximum transport velocity for each N source changes with the nutrient history (satisfying tables 1(v) and 1(vii)). Here we relate transport for each N source to the nutrient status as indicated by Q (cellular N:C ratio), giving a parameter Tq. The specific form of this response curve varies considerably between species but seems to fall into two basic patterns. Either there is an increase in Tq with declining Q (i.e. the more N starved the cell, the higher the potential transport rate of the nutrient), or (typically for nitrate) an initial increase followed by a decrease (e.g. Dortch *et al.* 1982; Syrett *et al.* 1986). The forms used, developed from curve fits to data for *Emiliania huxleyi* and *Heterosigma carterae* (work in preparation) are illustrated in figure 5 and defined in equation 5.1 for ammonium, giving NH4Tq, and equation 5.5 for nitrate, giving NO3Tq.

While the maximum transport rates at a given value of Q are set by NH4Tq and NO3Tq, those rates are then modified as a function of the concentration of the substrates (using a RH function) together with transport affinity constants (Ks), $NH4kT$ and $NO3kT$ in table 2. This satisfies table 1(vi). Transport is also controlled by the size of the internal nutrient pool of the substrate (using an inverse RH function) to halt transport when the internal pool attains a maximum value. Our data (in preparation and those of Dortch *et al.* (1984)) suggest that maximum pool sizes should be in the 10's to low 100's mM. Some others, such as DeManche *et al.* (1979) and Stolte & Riegman (1996) have suggested much larger pool sizes up into the low M range. Maximum pool sizes given in table 1 are set as 0.01 N:C (*ca.* 143 mM) for nitrate and 0.002 N:C (*ca.* 29 mM) for ammonium. Although the model will operate with high concentration pools we believe that they are unreasonable and sometimes impossible simply on solubility grounds.

Transport may also be moderated by an organic compound (e.g. Serra *et al.* 1978). There is a consensus of opinion that nitrogen metabolite repression of nitrate assimilation is regulated by an organic N compound which is probably an early product of N assimilation (Flynn 1991), such as glutamine (satisfying table 1(iv)). A positive correlation between a loss of nitrate assimilatory functions and high intracellular pools of glutamine has been shown (Syrett

Table 2. *Constants and their definitions. Italic parameters referred to in definitions are constants (elsewhere in this table), bold parameters are levels (table 3). Use of the constant is indicated by reference to other tables.*

constant	value	unit	definition	table
AAskGLN	0.001	N:C	Km for amino acid (AA) synthesis; substrate is GLN (i.e. **GLNP**)	7
Cresk	0.01	none	constant for computing C reserve	4
CresQ	0.2	N:C	value of **Q** when there is no reserve C for dark N assimilation	4
GLNPm	0.01	N:C	maximum GLN pool (**GLNP**) given *Qmax* of 0.2 N:C	6,7
GShGLN	0.01	none	Kh for GLN (i.e. **GLNP**) suppression of GS activity; relative to *GLNPm*	7
GSkNH4	1.75×10^{-5}	N:C	Km for GS activity; substrate is NH_4^+ (**NH4P**)	7
Kq	0.02	N:C	constant for control of growth rate from **Q**	7
NH4A	0.05	N:C·h^{-1}	constant for curve fit for NH4Tq	5
NH4hGLN	0.1	none	Kh for GLN (**GLNP**) suppression of NH_4^+ transport; relative to *NH4mGLN*	5
NH4hP	0.1	none	constant for NH_4^+ pool (**NH4P**) suppression of NH_4^+ transport; relative to *NH4Pm*	5
NH4kT	0.014	μg N ml^{-1}	Ks for NH_4^+ (i.e. **NH4**) transport rate	5
NH4mGLN	0.01	N:C	size of GLN pool (**GLNP**) which stops NH_4^+ transport	5
NH4Pm	0.002	N:C	maximum NH_4^+ pool (**NH4P**) given *Qmax* of 0.2 N:C	5
NO3A	−0.075	none	constant for curve fit for NO3Tq	5
NO3B	0.2	none	constant for curve fit for NO3Tq	5
NO3C	−0.4	none	constant for curve fit for NO3Tq	5
NO3hGLN	0.005	none	Kh for GLN (**GLNP**) suppression of NO_3^- transport; relative to *NO3mGLN*	5
NO3hP	0.05	none	Kh for NO_3^- (**NO3P**) suppression of NO_3^- transport; relative to *NO3Pm*	5
NO3kT	0.014	μg N ml^{-1}	Ks for NO_3^- (i.e. **NO3**) transport rate	5
NO3mGLN	0.003	N:C	size of GLN pool (**GLNP**) which stops NO_3^- transport	5
NO3Pm	0.01	N:C	maximum NO_3^- pool (**NO3P**) given *Qmax* of 0.2 N:C	5
NO3qmin	5.6	C:N	maximum $\mathbf{Q}^{-1}$ at which NO_3^- transport stops; constant for curve fit for NO3Tq	5
NNiRhGLN	0.01	none	Kh for GLN (i.e. **GLNP**) suppression of NNiR synthesis; relative to *GLNPm*	6
NNiRhNO3	0.01	none	Kh for NO_3^- pool (**NO3P**) induction of NNiR synthesis; relative to *NO3Pm*	6
NNiRhs	0.01	none	constant for control of NNiR synthesis; relative to NNiRm	6
NNiRkNO3	3.5×10^{-5}	N:C	Km for NNiR activity; substrate is NO_3^- (i.e. **NO3P**)	6
Qmax	0.2	N:C	maximum N:C (minimum C · N^{-1})	6,7
Qo	0.05	N:C	minimum N:C	7
Redco	2.28	N:C	mass of C respired for dark reduction of nitrate to ammonium	7
Umax	0.05	C · C^{-1} · h^{-1}	theoretical maximum C-specific growth rate	5–7

& Peplinska 1988). Consequently, we use GLN as an additional regulator of transport, using an inverse sigmoidal function. Different values of Kh have been assigned for nitrate and ammonium (*NO3hGLN* and *NH4hGLN*, table 2) because cells growing on ammonium have more GLN in them (Flynn 1991). Thus we derive transport rates for the two N sources, taking into account external and internal substrate concentrations and the presence of internal GLN, giving NH4T (equation 5.2) and NO3T (equation 5.6).

(c) *Nitrate reduction to ammonium (figures 2, 3; equation 6.x in table 6)*

Nitrate is the main form of oxidized N which accumulates in algae and the subsequent process of conversion through to intracellular ammonium is dependant on a supply of reductant which must come either from photosynthesis, or from the use of C reserves. Biochemically this process involves two enzymes (nitrate and nitrite reductases, NR and NiR, respectively) and two pools (nitrate and nitrite). Although much is known about nitrate reductase (Solomonson & Barber 1990; Campbell 1996), and microalgal NR has been studied for several decades (e.g. Eppley *et al.* 1969*a*; Everest *et al.* 1986), the regulation of nitrate assimilation in phytoplankton is not understood fully. However, the synthesis of the enzymes appears to be regulated by nitrate derepression and induction (e.g. Hipkin *et al.* 1983) and N-metabolite repression (reviewed by Solomonson & Barber (1990); Schnell & Lefebvre (1993)). Synthesis is repressed by the presence of an, as yet, unidenti-

Table 3. *Definition of levels, initial values and flows. Italic parameters in initial values are constants (table 2). References to the tabulated location of other definitions are given. Comments refer to the functionality of the adjacent part of the equation.*

level	unit	initial value	flow	definition and comment	table
C	µg C ml^{-1}	as required		algal carbon	
			+dt · dC	increase in cell C in suspension	7
GLNP	N:C	0 to *GLNPm*		internal glutamine pool	
			+dt · GS	increase by GS activity	7
			−dt · AAs	decrease by amino acid synthesis	7
			−dt · dGLNP	dilution with C growth	7
NH4	µg N ml^{-1}	as required		ammonium in growth medium	
			−dt · dNH4	removal from medium for cells	5
NH4P	N:C	0 to *NH4Pm*		internal ammonium pool	
			+dt · NH4T	increase by ammonium transport	5
			+dt · NO3red	increase from nitrate reduction	6
			−dt · GS	decrease by GS activity	7
			−dt · dNH4P	dilution with C growth	5
NO3	µg N ml^{-1}	as required		nitrate in growth medium	
			−dt · dNO3	removal of nitrate from medium for cells	5
NO3P	N:C	0 to *NO3Pm*		internal nitrate pool	
			+dt · NO3T	increase by nitrate transport	5
			−dt · NO3red	decrease from nitrate reduction	6
			−dt · dNO3P	dilution with C growth	5
NNiR	N:C·h^{-1}	0 to *Umax*·*Qmax*		nitrate–nitrite reductase activity	
			+dt · NNiRs	increase in activity by synthesis	6
			−dt · NNiRd	decrease in activity by decay and dilution with C growth	6
Q	N:C	*Qo* to *Qmax*		cell N:C mass ratio	
			+dt · AAs	increase by amino acid synthesis	7
			−dt · dQ	dilution with C growth	7

Table 4. *Control of operation in the dark. Italic parameters in definition are constants (table 2), bold parameters are levels (table 3). Comments refer to the functionality of the adjacent part of the equation.*

equation	auxiliary	unit	definition	comment
4.1	PS	none	1 if light; 0 if dark	control of LD cycle; link to simulation run time. Relate to normalized PI curve if required (see text)
4.2	Creserv	none	$\dfrac{\left(1-\dfrac{\mathbf{Q}}{CresQ}\right)^4}{\left(1-\dfrac{\mathbf{Q}}{CresQ}\right)^4+Cresk}$	quotient for availability of C in darkness
4.3	NRreduc	none	PS + 0.6 · Creserv	quotient for availability of C to support NNiR activity. Only if (PS + 0.6 · Creserv) < 1, else NRreduc = 1
4.4	CGOGAT	none	PS + Creserv	quotient for availability of C for GS activity. Only if (PS + Creserv) < 1, else CGOGAT = 1
4.5	CAAs	none	PS + Creserv	quotient for availability of C for AA synthesis. Only if (PS + Creserv) < 1, else CAAs = 1

fied organic compound which is most likely an early product of inorganic N assimilation (Solomonson & Barber 1990). In addition, the enzymes are subject to protein turn over (Sherman *et al.* 1983; Valasco *et al.* 1988). The model thus needs to simulate all these steps.

For simplicity, the process of nitrate reduction through to ammonium has been treated as one process (Faure *et al.* (1991) suggest that *NR* and *NiR* may be co-regulated), with the total activity of nitrate–nitrite reductase termed NNiR. Enzyme activity cannot exceed a value which would support the maximum growth rate, *Umax*, with the maximum N:C ratio, *Qmax* (equation 6.2); it is possible that in reality activity could exceed this value on occasion. Synthesis of NNiR is induced (promoted) by the concentration of the internal nitrate pool (satisfying table 1(xiv)) and repressed by the organic N metabolite pool (GLN) using sigmoidal functions (equation 6.3). There is a decay function (equation 6.6, normalized to *Umax*) to decrease the enzyme activity. The actual rate of reduction of nitrate (NO3red) is then a

Table 5. *Control of ammonium and nitrate transport. Italic parameters in definition are constants (table 2), bold parameters are levels (table 3). Comments generally refer to the functionality of the adjacent part of the equation.*

equation	auxiliary	unit	definition	comment
5.1	NH4Tq	N:C·h^{-1}	$(NH4A - 0.2 \cdot \mathbf{Q}) \cdot \frac{Umax}{0.05}$	maximum ammonium transport at given value of **Q**. Normalized to *Umax*
5.2	NH4T	N:C·h^{-1}	$\mathrm{NH4Tq} \cdot \frac{\mathbf{NH4}}{(\mathbf{NH4} + NH4kT)}$	ammonium transport related to substrate (**NH4**) concentration
			$\cdot \frac{\left(1 - \frac{\mathbf{NH4P}}{NH4Pm}\right)}{\left(1 - \frac{\mathbf{NH4P}}{NH4Pm}\right) + NH4hP}$	decreases with size of **NH4P**
			$\cdot \frac{\left(1 - \frac{\mathbf{GLNP}}{NH4mGLN}\right)^4}{\left(1 - \frac{\mathbf{GLNP}}{NH4mGLN}\right)^4 + NH4hGLN}$	decreases with size of **GLNP**. Only if **GLNP** $< NH4mGLN$, else NH4T = 0
5.3	dNH4	µg N ml^{-1} · h^{-1}	$\mathrm{NH4T} \cdot \mathbf{C}$	removal of ammonium from medium
5.4	dNH4P	N:C·h^{-1}	$\mathrm{Cmu} \cdot \mathbf{NH4P}$	correction of **NH4P** with Cmu (table 7)
5.5	NO3Tq	N:C·h^{-1}	$NO3A \cdot (1 - \mathrm{e}^{NO3B((1/\mathbf{Q}) - NO3q_{\min})}) \cdot \mathrm{e}^{NO3C((1/\mathbf{Q}) - NO3q_{\min})} \cdot \frac{Umax}{0.05}$	maximum nitrate transport at given value of **Q**. Normalized to *Umax*. Only if $NO3qmin < 1/\mathbf{Q}$, else NO3Tq = 0
5.6	NO3T	N:C·h^{-1}	$NO3Tq \cdot \frac{\mathbf{NO3}}{\mathbf{NO3} + NO3kT}$	nitrate transport related to substrate (**NO3**) concentration
			$\cdot \frac{\left(1 - \frac{\mathbf{NO3P}}{NO3Pm}\right)}{\left(1 - \frac{\mathbf{NO3P}}{NO3Pm}\right) + NO3hP}$	decreases with size of **NO3P**
			$\cdot \frac{\left(1 - \frac{\mathbf{GLNP}}{NO3mGLN}\right)^4}{\left(1 - \frac{\mathbf{GLNP}}{NO3mGLN}\right)^4 + NO3hGLN}$	decreases with size of **GLNP**. Only if **GLNP** $< NO3mGLN$, else NO3T = 0
5.7	dNO3	µg N ml^{-1} · h^{-1}	$\mathrm{NO3T} \cdot \mathbf{C}$	removal of nitrate from medium
5.8	dNO3P	N:C·h^{-1}	$\mathrm{Cmu} \cdot \mathbf{NO3P}$	correction of **NO3P** with Cmu (table 7)

function of the level of NNiR, a RH function of the size of the nitrate pool using a Km for nitrate reductase equivalent to 500 µM (this is at the high end of literature values (e.g. Syrett 1981; Berges & Harrison 1995)) and also of the availability of reductant (NRreduc, equation 4.3). This gives equation 6.4 as the rate of nitrate reduction to ammonium. There is no evidence for a rapid and direct negative feedback of the reduction process by an organic compound (table 1(xvi)) and no such link is used here. However, it is possible that through competition for reductant (especially in darkness and during ammonium feeding) the assimilation of N into amino acids and beyond may have implications for nitrate–nitrite reduction (Turpin 1991). The current model does not attempt to mimic any such interactions except that assimilation of ammonium decreases Creserv (equation 4.2) and thus affects the operation of NO3red (equation 6.4) via the availability of reductant (equation 4.3).

Note that the level NNiR has units of enzyme activity (analogous to that determined by *in vitro* enzyme assay), rather than mass. Based on a turnover number (Kcat) of 500 s^{-1} and a molecular mass of 200 kD for functional, dimeric NR (Hipkin 1989) and a Kcat of 50 s^{-1} with mass of 60 kD for NiR (Wray 1989), we calculate that the contribution of NR and NiR to cell nitrogen is less than 0.03% with cells growing with *Umax* and *Qmax* as given in table 2. The actual amount of NR and NiR enzyme as a pro-

Table 6. *Nitrate reduction through to ammonium. Italic parameters in definition are constants (table 2), bold parameters are levels (table 3). Comments generally refer to the functionality of the adjacent part of the equation.*

equation	auxiliary unit	definition	comment	
6.1	NNiRms	N:C·h^{-1}	$1.2 \cdot Umax \cdot Qmax$	maximum **NNiR** synthesis; normalized to *Umax* and *Qmax*
6.2	NNiRm	N:C·h^{-1}	$Umax \cdot Qmax$	maximum **NNiR** activity
6.3	NNiRs	N:C·h^{-1} · h^{-1}	$\mathrm{NNiRms} \cdot \frac{(\mathrm{NNiRM} - \mathbf{NNiR})}{(\mathrm{NNiRm} - \mathbf{NNiR} + NNiRhs)}$	synthesis of **NNiR** activity. Limited to *NNiRm*
			$\frac{\left(\frac{\mathbf{NO3P}}{NO3Pm}\right)^2}{\left(\frac{\mathbf{NO3P}}{NO3Pm}\right)^2 + NNiRhNO3}$	induced by size of **NO3P**
			$\frac{\left(1 - \frac{\mathbf{GLNP}}{0.3 \cdot GLNPm}\right)^4}{\left(1 - \frac{\mathbf{GLNP}}{0.3 \cdot GLNPm}\right)^4 + NNiRhGLN}$	suppressed by size of **GLNP**. Only if $\mathbf{GLNP} < 0.3 \cdot GLNPm$, else NNiRs = 0
6.4	NO3red	N:C·h^{-1}	$NNiR \cdot \frac{\mathbf{NO3P}}{(\mathbf{NO3P} + NNiRkNO3)}$	reduction of nitrate to ammonium increases with substrate (**NO3P**)
			·NRreduc	depends on availability of C in darkness (table 4)
6.5	NNiRdr	h^{-1}	$1.2 \cdot Umax$	decay rate constant for **NNiR**; normalized as 20% higher than *Umax*
6.6	NNiRd	N:C·h^{-1} · h^{-1}	$\mathbf{NNiR} \cdot (\mathrm{NNiRdr} + \mathrm{Cmu})$	decay rate of **NNiR** activity together with correction of activity with Cmu (table 7)

portion of total cell N is thus considered to be negligible and the drain on resources is not simulated.

(*d*) *Assimilation of intracellular ammonium and growth (figures 2, 3; equation 7.x in table 7)*

The first organic product of N assimilation (via the glutamate synthase cycle (Syrett 1981; Robertson & Alberte 1996)) is GLN. In the model we refer explicitly to glutamine synthetase (GS) and to the GLN pool. Glutamine synthetase is a constitutive enzyme which is regulated by end product inhibition (Akimova *et al.* 1976; Miflin & Lee 1980) involving GLN (satisfying table 1(xv)). Maximum GS activity (GSm, equation 7.1) is set by $Umax \cdot Qmax$ (as was the maximum NNiR activity). GS activity is made a RH function of substrate concentration (i.e. the size of NH4P) using a Km value equivalent to 250 µM (at the high end of literature values (e.g. Syrett 1981; Clayton & Ahmed 1987; Ahmed & Hellebust 1988)). GS activity is also an inverse sigmoidal function of the GLN pool to achieve product inhibition and also a function of the availability of C (CGOGAT) for assimilation of inorganic N in the dark (equation 7.2). The maximum pool size for GLN ($GLNPm = 0.01$ N:C, table 2) is equivalent to *ca.* 72 mM which is at the higher range of those reported in the literature (e.g. Flynn *et al.* 1993; Wood & Flynn 1995). Like all maximum pool values, $GLNPm$ can be readily altered as regulatory functions from pools are normalized to maximum pool values, although the absolute value of the nutrient pool will still affect reaction rates through Michaelis–Menten kinetics.

The next step is the use of GLN-N for amino acid synthesis, AAs, and thereafter for nucleic acid synthesis and protein synthesis (figure 3). Again, the maximum rate (AAsm, equation 7.4) is fixed by $Umax \cdot Qmax$. AAs has been made a RH function of the size of the GLN pool and also of the availability of C in darkness (equation 7.5). The rate of flow of N through amino acid synthesis is also made a function of the current nutrient status of the cell (as defined by Q), on the basis that a N-starved cell will not have the biochemical machinery to perform all processes at maximum rates. If this is not included then the model does not simulate the rapid increase in GLN (level GLNP) seen when N-starved cells are refed (Flynn *et al.* 1989). Another consequence of this modification is that the lag phase becomes longer as N starvation increases (Q approaching the minimum value, Qo, something which is usually apparent in batch culture experiments. However, an additional

Table 7. *Control of Gln, Q and cell growth. Italic parameters in definition are constants (table 2), bold parameters are levels (table 3). Comments generally refer to the functionality of the adjacent part of the equation.*

equation	auxiliary unit	definition	comment	
7.1	GSm	N:C·h^{-1}	$Umax \cdot Qmax$	maximum GS activity
7.2	GS	N:C·h^{-1}	$\mathrm{GSm} \cdot \frac{\mathbf{NH4P}}{\mathbf{NH4P} + GSmNH4}$	GLN synthesis related to substrate (**NH4P**) concentration
			$\cdot \frac{\left(1 - \frac{\mathbf{GLNP}}{GLNPm}\right)^4}{\left(1 - \frac{\mathbf{GLNP}}{GLNPm}\right)^4 + GShGLN}$	decreases with size of **GLNP**
			·CGOGAT	depends on availability of C in darkness (table 4)
7.3	dGLNP	N:C·h^{-1}	$\mathrm{Cmu} \cdot \mathbf{GLNP}$	correction of **GLNP** with Cmu
7.4	AAsm	N:C·h^{-1}	$Umax \cdot Qmax$	maximum amino acid synthesis
7.5	AAs	N:C·h^{-1}	$\mathrm{AAsm} \cdot \frac{\mathbf{GLNP}}{\mathbf{GLNP} + AAskGLN}$	amino acid synthesis related to substrate (**GLNP**) concentration
			$\cdot \frac{\mathbf{Q} - Qo}{\mathbf{Q} - Qo + Kq} \cdot \left(2 - \frac{\mathbf{Q} - Qo}{Qmax - Qo}\right)$	changes as a function of **Q**
			·CAAs	depends on availability of C in darkness (table 4)
7.6	resp	C · C^{-1} · h^{-1}	$Redco \cdot \mathrm{NO3red}$	respiration to support reduction of nitrate to ammonium. Only if PS = 0, else resp = 0
7.7	Cmu	C · C^{-1} · h^{-1}	$\mathrm{PS} \cdot Umax$	C growth linked to light,
			$\cdot \frac{\mathbf{Q} - Qo}{\mathbf{Q} - Qo + Kq}$	and **Q**,
			−resp	corrected for respiration
7.8	dC	µg C ml^{-1} · h^{-1}	$\mathrm{Cmu} \cdot \mathbf{C}$	increase in cell C with C growth
7.9	dQ	N:C·h^{-1}	$\mathrm{Cmu} \cdot \mathbf{Q}$	decrease of **Q** with C growth

term, $(2-(\mathrm{Q}-\mathrm{Qo})/(Qmax-\mathrm{Qo}))$, has been included in the definition of AAs (equation 7.5) which ensures that amino acid synthesis is raised when Q is close to Qo. Without this term, the lag phase can become unreasonably long. The equation used gives lag phases when Q ≈ Qo of a few days, which in our experience is of the correct magnitude.

The part of the model simulating growth (in terms of C, Cmu in equation 7.7) is modified from a conventional cell-quota model (Caperon 1968*a*, *b*; Droop 1968). The only difference is that the N uptake component is now replaced with the transfer of N through from the GLN pool. Amino acid synthesis will affect the rate at which N (as nitrate and/or as ammonium) enters the system by feedback through the previous stages. This could be viewed as being more realistic as growth is now a function of the amount of organic N present in the cell (i.e. of the amount of protein, enzymes, nucleic acids, etc.) rather than of total N (including internal pools of inorganic N). It should be noted that *Umax* is a theoretical maximum growth rate; depending on the value of Kq, and hence the shape of the curve relating Cmu to Q, the

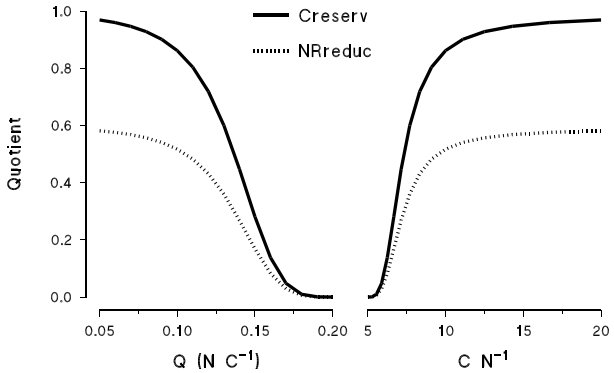

Figure 4. Form of functional relationships between Creserv and NRreduc with Q giving the quotient needed to correct process rates (table 4). The plot is also given in relationship to the cellular C · N^{-1} ratio (i.e. Q^{-1}).

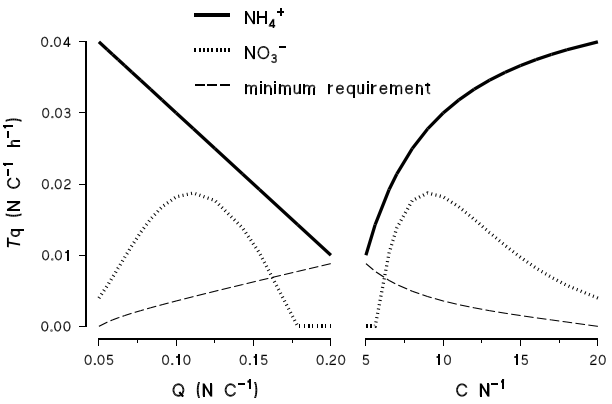

Figure 5. Form of functional relationships between Tq and Q for the maximum potential ammonium and nitrate transport rates (equations 5.1 and 5.5 in table 5). The equation for nitrate (NO3Tq), equation 5.5, relates Tq to $C{\cdot}N^{-1}$ because the form of the equation used fitted experimental data better than relating it to Q. The minimum transport requirement is determined from $Tq = Cmu \cdot Q$, where Cmu is derived from Q using parameters in table 2 and equation 7.7 in table 7. The difference between the minimum requirement and the potential rate is indicative of the level of excess transport possible when cells are N stressed (i.e. Q is low).

value of Cmu at *Qmax* may be closer or further from *Umax*. The values of NNiRm (equation 6.2), GSm (equation 7.2) and AAsm (equation 7.4) are all set at $Umax{\cdot}Qmax$; changing these values will affect the value of Cmu and/or sizes of the preceding nutrient pool (NO3P, NH4Pand GLNP, respectively).

(*e*) *Operation in light–dark cycles*

To enable a simulation of events that occur in darkness, a clock function may be included as a switch (analogous to lights being switched on or off) which alters the relative rate of photosynthesis (value of PS, equation 4.1) and hence of the C-specific growth rate Cmu (equation 7.7). PS may also be altered between 0 and 1 according to a normalized photosynthesis–irradiance (P–I) curve if required. The P–I curve we have used (after Jassby & Platt 1976) is described by

$$PS = \tanh(\alpha \cdot PFD),$$

where α has been set at 0.01 and PFD is the irradiance as a photon flux density. With the inclusion of a sine curve function to give a more natural transition between light and dark, with a peak PFD of 500 μmol m^{-2} s^{-1} at 6 h into the day, we obtain a value of PS > 0.95 (at PFDs above 200 μmol m^{-2} s^{-1}) during the middle 8 h of the 12:12 h L:D cycle. These relationships may be readily altered as required. It should be possible to combine the current model with that of Geider *et al.* (1996) so simulating photoadaptation and other interactions (Osborne & Geider 1986).

Cmu is corrected for the use of C for the dark reduction of nitrate through to ammonium (equation 7.7). This process requires $8e^{-}(NAD(P)H_2 + 6Fe_{red})$, equivalent to $4NAD(P)H_2$ per molecule of nitrate. In the presence of light, all reductant is considered to be photogenerated. In darkness, we assume that heterotrophically generated $NAD(P)H_2$ can also be used to generate reduced ferredoxin. Thus, in the dark, reductant may be generated from hexose using the pentose phosphate pathway, or from fatty acids using β oxidation and entry of acetyl-CoA into the TCA cycle. Both these routes would require oxidation of 2C to give the $4NAD(P)H_2$ required to reduce each NO_3^- to NH_4^+. As a mass ratio this equates to the loss (respiration) of 1.71 g C per 1 g nitrate N reduced to ammonium; this value has been used (*Redco*, table 2) to compute the respiratory loss in the dark (resp., equation 7.6). Housekeeping respiration (which may vary with Cmu (Laws & Caperon 1976)), and that associated with the assimilation of intracellular ammonium (whether from nitrate or otherwise), is considered to be the same irrespective of the nitrogen source being supplied and is not accounted for. At this stage, we feel that in order to model ammonium and nitrate assimilation interactions it is unnecessary to model the levels of C metabolism indicated in works such as Turpin *et al.* (1988) in such detail.

(*f*) *Parametrization*

Although there is no single data set published for any species of phytoplankton with which to parametrize this model, of the 30 constants listed in table 2, two thirds may be derived relatively easily from various experimental investigations (although it should be noted that this would not be a trivial undertaking). Transport and enzyme affinity constants have been estimated from the literature (as indicated above) and from other experimental data (Flynn *et al.* 1997). The main problem is the functional form of the response curves for the inter-pool relationships, the constants for which comprise the remaining third of the constants in table 1. The sensitivity of these curves to different constants is considered in § 3.

3. RESULTS

For the purposes of this paper, two types of results are presented: firstly, a demonstration that the model can simulate facets of ammonium–nitrate interactions as detailed in table 1; and secondly, a sensitivity analysis on the values of parameters and response curves for which biological data are scarce or unavailable. Reference to the *f*-ratio indicates the proportion of nitrogen taken up as nitrate, with $f = 1$ when nitrate is the sole form transported and $f = 0$ when using only ammonium. Using the parameters of the model,

$$f = \frac{NO3T}{(NH4T + NO3T)}.$$

(*a*) *Simulation of ammonium–nitrate interactions*

Figure 6 simulates an experiment in which cells have been grown exponentially and then subjected

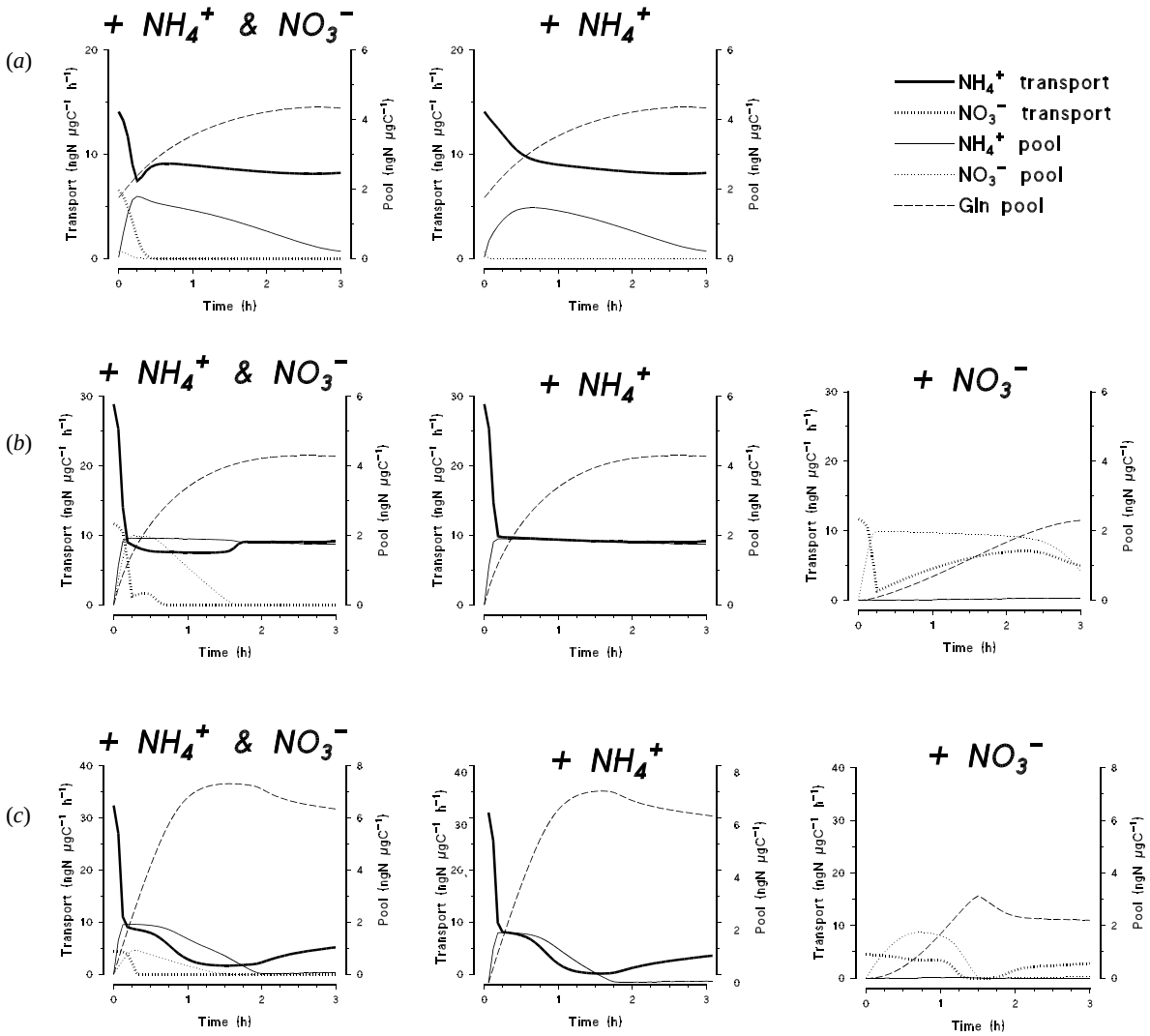

Figure 6. Simulation of a refeeding experiment in which cells were grown exponentially on ammonium or nitrate, N starved for different periods and then refed (all additions of 1.4 µg N ml^{-1} (= 100 µM)). The model is as described in tables 2–7, except that the maximum pools of both nitrate and ammonium ($NO3Pm$ and $NH4Pm$) are set equal at 0.002 N:C (= 28.6 mM). (*a*) Exponentially growing cells using nitrate and then supplied with ammonium as well, or with the nitrate removed and ammonium added. (*b*) Ammonium-grown cells after 24 h of N starvation; and (*c*) after 48 h of N starvation with the additions indicated. Note the different vertical scales used.

to various periods of N deprivation. Samples were supplied with ammonium and/or nitrate. Such experiments are typical of those conducted by Syrett and co-workers (e.g. Cresswell & Syrett 1979; Hipkin & Syrett 1977; Syrett *et al.* 1986). Cells growing exponentially on ammonium did not show any capability to take up nitrate (not shown, satisfies table 1(ii)) but had to undergo a period of starvation (a few hours) until GLN and Q had fallen sufficiently to enable transport of nitrate and then induction of NNiR. Nitrate-growing cells (figure 6*a*) took up ammonium immediately when ammonium and nitrate were available together (with a rapid cessation of nitrate transport over 20 min), or when ammonium was supplied alone. This satisfies table 1(iii). Cells starved of N for 24 h (figure 6*b*) took up both ammonium and/or nitrate. Under these conditions transport of ammonium was more rapid, resulting in a very rapid increase in intracellular GLN. When ammonium and nitrate were supplied together there was a brief period of nitrate transport, with the nitrate pool being depleted after nitrate transport stopped. This occurs because GLN suppresses nitrate transport and NNiR synthesis but not reduction itself (satisfying table 1(xv)). After 48 h of N deprivation, the situation is similar to that seen at 24 h, except that initial ammonium transport is more rapid and nitrate transport slower. In all N deprivation simulations, ammonium transport rates declined rapidly after the first few minutes, whereas nitrate transport into cells supplied with nitrate alone was delayed in accordance with the induction of NNiR synthesis (i.e. a decoupling of nitrate transport and reduction occurs (Collos 1982, 1983)). All of these observations satisfy the requirements of table 1(vi), (vii), (ix) and (x).

Figures 7 and 8 simulate growth in cultures (in continuous light or in a L:D cycle, respectively) where the inoculum of N deprived cells is small and there is a continuous low dilution of the culture with fresh

media. This 'stretch-batch' system results in a period of exponential growth (as in a batch system) which is prolonged due to dilution, a period of increasing N stress and, eventually, a steady-state growth at low growth rate. Both systems show similar patterns of a high initial rate of ammonium transport. In addition, there is an initial but brief transport of nitrate similar to that seen in figure 6*c* (but not clear in figures 7, 8 at the scale plotted), an increase in N:C (i.e. in Q), high GLN levels during growth on ammonium and a subsequent rise in the *f*-ratio as external ammonium concentrations decline and transport switches towards nitrate. Q is slightly higher during growth on ammonium with little difference in growth rates, satisfying tables 1(viii) and (xii). In the L:D simulation (figure 8*b*), there is a diel oscillation of the *f*-ratio because nitrate assimilation (and hence transport) is adversely affected by the absence of light for cells with little C reserve. Cells in darkness thus make greater proportionate use of the ammonium which is continuously entering the system, hence decreasing the *f*-ratio. Eventually the *f*-ratio reflects the proportions of the nutrients in the feed media. The complications of operating in a L:D cycle are apparent in comparing the two systems. The oscillations in the simulation are present when the light is either switched on or off abruptly, and also when the PFD is related to a sine curve, as in figure 8. What is not apparent at the scale plotted is that the transport of ammonium and nitrate is no longer coupled with the L phase as the cells become increasingly N stressed beyond 200 h in figure 8. This link between N status and coupling–decoupling of light and N assimilation is seen more clearly in the simulation shown in figure 9.

Figure 9 simulates a situation where N stress in cells is relieved by using a dilution rate above that equivalent to the maximum growth rate in a L:D cycle. This shows the effect of changes in the N status (in Q) and L:D cycle on the use of nitrate and ammonium. Initially (before 72 h), both nitrate and ammonium are used equally and throughout the L:D cycle. As the washout proceeds, the residual external nutrient concentrations rise and the cellular N:C ratio (Q) also rises (figure 9*a*). Because of the preference for ammonium, coupled with a decrease in the availability of C for CGOGAT, CAAs and reductant in the dark for N assimilation, there is a progressive shift towards the use of ammonium and a gradual loss of the ability to uncouple N assimilation and C growth (photosynthesis) in the dark as the N status of the cells improves. This satisfies tables 1(i), (xi) and (xiii). Note that internal pools of ammonium and nitrate (until nitrate transport halts completely beyond 240 h) are near maximal in the dark and also the presence of characteristic peaks of GLN which appear when the lights come back on (e.g. Flynn *et al.* 1993).

(*b*) *Sensitivity analysis*

For this purpose a common test procedure was followed in which the external nitrate concentration was

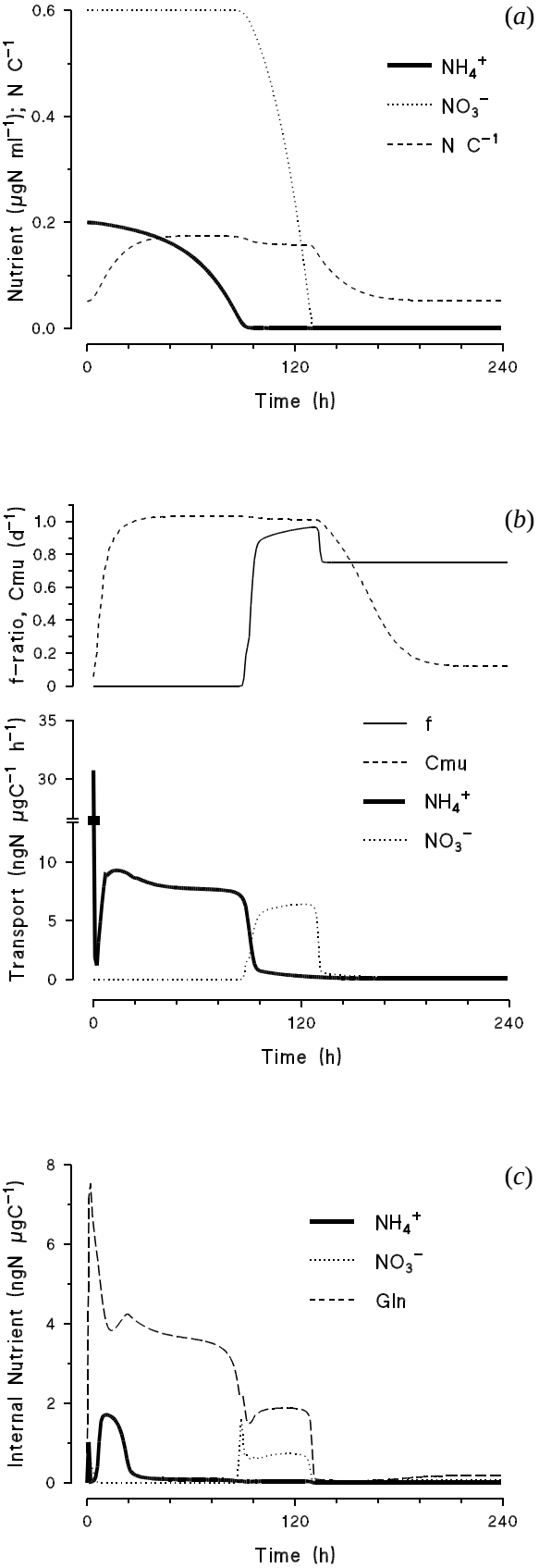

Figure 7. Simulation of a 'stretch-batch' culture (see text) grown in continuous light with a dilution rate of 0.005 h^{-1} supplied with 0.2 μg N ml^{-1} (14.28 μM) of ammonium and 0.6 μg N ml^{-1} (42.9 μM) of nitrate. External nutrients and N:C ratio (Q) of the cells (*a*); transport rates of ammonium and nitrate together with the *f*-ratio and C-specific growth rate (*b*); and internal nutrient pools of nitrate, ammonium and GLN (*c*).

PHILOSOPHICAL TRANSACTIONS OF THE ROYAL SOCIETY B BIOLOGICAL SCIENCES

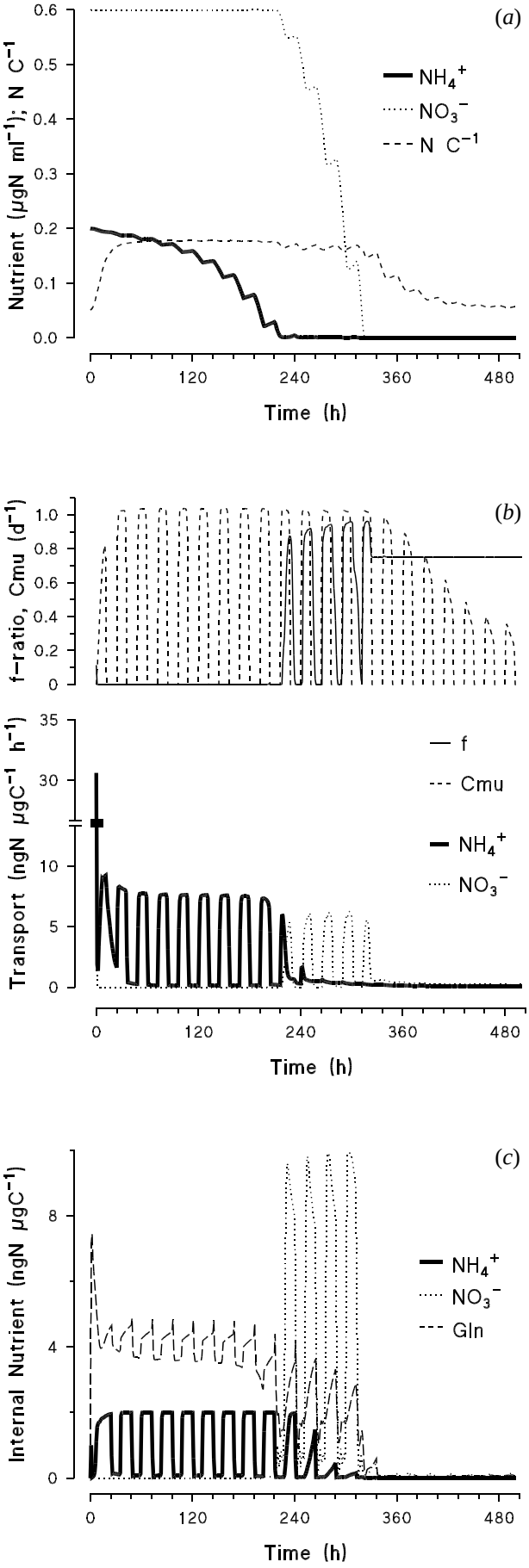

Figure 8. As figure 7 but with light supplied in a 12 h:12 h light:dark cycle using a sine curve to describe changes in the photon flux density between 0 and 500 μmol m^{-2} s^{-1}. Values of PS were computed as described for figure 10.

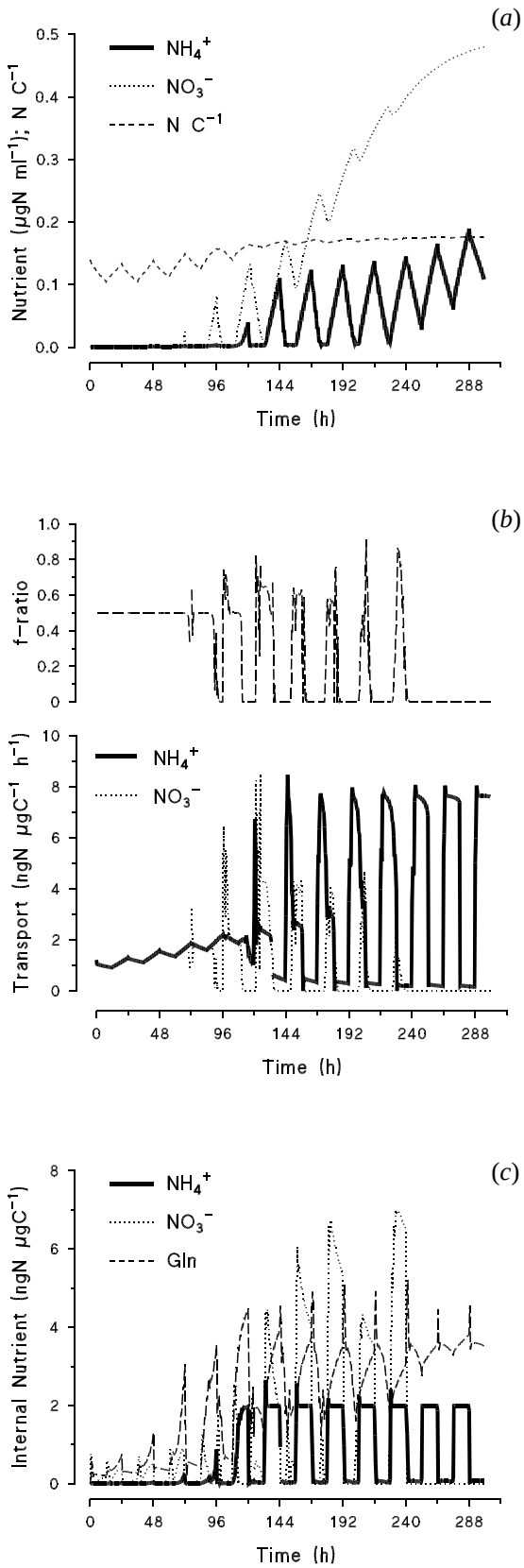

Figure 9. Simulation of a culture grown under N-limiting conditions which is gradually relieved of N stress through slow washout (use of dilution rate exceeding growth rate) while growing in a 12 h:12 h light:dark cycle (PS either being equal to 1 or 0). The nutrients were supplied at 0.5 μg N ml^{-1} (35.7 μM) each of nitrate and ammonium. External nutrients and N:C ratio (Q) of the cells (*a*); transport rates of ammonium and nitrate together with the *f*-ratio and C-specific growth rate (*b*); and internal nutrient pools of nitrate, ammonium and GLN (*c*).

maintained at an excess of 1.4 μg N · ml^{-1} (100 μM) and the concentration of ammonium varied in order to attain various steady-state f-ratios while using different values for the test parameter. In addition, in order to test only the post-transport processes, Tq values were fixed rather than related to the N status through Q. The model was run to steady state at a required f-ratio and single parameter sensitivity indices (S) have been computed according to the equation

$$S = \frac{(Ra - Rc)/Rc}{(Pa - Pc)/Pc},$$

where Ra and Rn are model responses for the altered and control parameters and Pa and Pn the altered and control parameter values. The results using data with the f-ratio set at 0.5 (i.e. equal use of both N sources) are presented in table 8. These are steady-state results (defined by a stable value for Q), although some of the conditions give rise to oscillations in some levels (notably NO3P) when the target f is set at 0.5; stable results are given at, for example, $f = 0.25$ or 0.75. Parameter changes giving values of $S \approx 0$, suggesting stability of the response in steady state, may often give significant changes in temporal responses to transient events. The constant values (given in table 2) chosen as defaults give the best all-round result.

The size of the nitrate pool (NO3P) was most sensitive to alteration in constants, reflecting the complexity of the associated regulatory processes. The most sensitive constant was found to be $NO3hGLN$ (tables 2, 8). If this was high then the shallow response curve (see figure 1, Kh = 0.01) resulted in NO3P being only part filled, while high values resulted in a pool which was usually almost full. Only with Kh values around 0.005 did the size of the pool reflect the proportion of N flowing through it, as one may expect by intuition. With this value of Kh, there is a degree of stable oscillation in nitrate transport and assimilation due to the complex feedback links.

Different Km values for the enzymic process regulated by Michaelis–Menten kinetics, namely nitrate reduction ($NNiRkNO3$), glutamine synthetase ($GSkNH4$) and $AAskGLN$, affect the sizes of the nitrate and ammonium pools, respectively, but otherwise have little effect. Lower values result in smaller pool sizes during nutrient-limited simulations, needing smaller integration steps and thus longer simulations. It is for this reason that the values for these parameters given in table 2 are at the upper end of the those recorded in the literature.

4. DISCUSSION

Several extensive reviews have appeared on the subject of nitrate–ammonium interactions in phytoplankton (Syrett 1981; Wheeler 1983; Dortch 1990), together with various schematic models of the regulation of N assimilation (e.g. Solomonson & Spehar 1977; Serra *et al.* 1978). However, attempts to formalise the interaction into a single coherent mathematical argument are limited. Previous attempts (e.g. DeManche *et al.* 1979; Stolte & Riegman 1996; R. A. Armstrong, personal communication) have been directed towards an examination of a specific process and/or are incapable of simulating key features of the interaction under transient conditions in which cell growth is also simulated. Flynn (1991) suggested a modelling strategy based on our understanding of the biochemistry of algal physiology and here we have attempted to construct such a model. The current model emphasizes interactions between the N sources and is not an exact simulation of biochemical reality. In certain areas, most notably the linkage between C and N metabolism (Beardall & Raven 1990; Turpin 1991), the current model is limited, though inclusion of such detail may not significantly improve the simulation of the interaction.

The need for a general model describing ammonium–nitrate interactions exists at several levels. Firstly, the ammonium–nitrate interaction is complex, varying with nutrient history (which changes during the course of N deprivation and during N assimilation) and with light. The underlying biochemical processes are complex and interconnected; even the study of transport into the cell has proved to be difficult because assimilation occurs so soon after entry ('uptake' invariably describes transport plus initial assimilation). Aspects of the interactions between the kinetics of nutrient transport and growth are considered by McCarthy (1981). Models offer an alternative route to investigate permutations of these processes which would otherwise take years to consider using experimental methods.

Secondly, it is difficult to study the interactions of these nutrients at very low substrate concentration (especially for ammonium which becomes increasingly difficult to monitor as concentrations decrease below 0.5 μM because of analytical problems associated with the presence of airborne ammonia in land-based laboratories) and at the low biomass levels required to mimic oceanic systems because of logistic problems of growing large volume cultures. We will present simulations of the ammonium–nitrate interaction under oceanic conditions in a future paper.

Thirdly, it is important to be able to model the use of nitrate and ammonium adequately in ecosystem models. Current ecosystem models incorporating ammonium–nitrate interactions often treat the algal cell as a 'black box'. They may relate the differential use of nitrate and ammonium to the external nutrient concentrations alone (Harrison *et al.* 1982; Collos 1989), using simple inhibition terms to achieve a switching between ammonium and nitrate (Fasham 1993; Parker 1993). Such models cannot simulate the transient changes in uptake which occur with changes in nutrient status and irradiation, which form such an important part of the interaction.

The test of the current model has been to see if it could simulate the types of responses which algal physiologists have reported from experiments conducted with a wide range of algae and experimental protocols. Fitting the model to a specific set of parameters for a named organism was not the aim. Our model simulates all the aspects listed in table 1, both

PHILOSOPHICAL TRANSACTIONS OF THE ROYAL SOCIETY B BIOLOGICAL SCIENCES

Table 8. *Sensitivity analysis*

(Tq values have been replaced with constants equivalent in the controls to 2(*Umax*·*Qmax*) and the external concentration of nitrate set at an excess value of 1.4 μg N ml^{-1} (100 μM). Ammonium concentrations were varied in order to attain an *f*-ratio of 0.5 (i.e. nitrate use equals ammonium use; default control conditions required 0.0049 μgN ml^{-1} = 0.35 μM ammonium). This table presents values of the single parameter sensitivity index S (see text) for the ammonium concentration at $f = 0.5$ together with S for the internal pools. The sign of S indicates the direction of the change in the model response with the parameter change, e.g. a doubling of response with a doubling of the parameter gives S = 1, a halving of the response with a doubling of the parameter gives S = −0.5.)

parameter		response; single parameter sensitivity index					
constant (and control value)	test values	NH4 for $f = 0.5$	NO3P	NNiR	NH4P	GLNP	Q
Tq ratio	2:4	−0.58	0.00	0.00	0.02	0.00	0.00
(NO3Tq:NH4Tq of 2)	1:2	0.10	1.12	−0.04	0.08	0.12	0.02
Ks ratio (μM:μM)	1:2	1.01	0.00	0.00	0.00	0.00	0.00
(*NO3kT*:*NH4kT* of 1:1)	1:0.5	1.00	0.00	0.00	0.00	0.00	0.00
NO3Pm (0.01 N·C^{-1})	0.005	−0.02	0.94	−0.02	−0.04	0.00	0.00
	0.020	0.01	0.89	−0.02	0.02	0.00	0.00
	0.040	0.00	0.84	−0.01	0.01	0.00	0.00
NO3hGLN (0.005)	0.0001	−0.08	−5.20	0.06	−0.04	−0.02	0.00
	0.0010	−0.01	−6.18	0.07	−0.05	−0.02	0.00
	0.0100	−0.04	−0.48	0.01	−0.02	−0.04	−0.01
NNiRhGLN (0.01)	0.001	0.01	0.71	−0.04	−0.02	0.00	0.00
	0.100	0.00	0.19	−0.00	0.00	0.00	0.00
NNiRkNO3	0.7×10^{-5}	0.00	0.05	0.03	0.00	0.00	0.00
(3.5×10^{-5} N·C^{-1})	18.0×10^{-5}	0.00	−0.24	−0.08	0.00	0.00	0.00
NH4hGLN (0.10)	0.001	0.29	0.00	0.00	−0.02	0.00	0.00
	0.010	0.30	0.00	0.00	−0.02	0.00	0.00
GSkNH4	0.35×10^{-5}	0.00	0.00	0.00	0.99	0.00	0.00
(1.8×10^{-5} N·C^{-1})	8.8×10^{-5}	0.00	0.00	0.00	1.05	0.00	
GShGLN (0.01)	0.001	0.00	0.00	0.00	0.09	0.00	0.00
	0.100	−0.01	0.03	0.01	0.24	−0.01	0.00
AAskGLN	0.0002	−0.08	−0.61	−0.34	−1.74	0.03	−0.18
(0.001 N·C^{-1})	0.0050	−0.13	−0.05	−0.11	−0.19	0.01	−0.09
Umax (0.05 h^{-1})	0.010	0.00	0.46	1.00	−0.03	0.00	0.00
	0.025	0.00	0.46	1.00	−0.02	0.00	0.00
	0.100	0.01	1.40	0.95	0.00	0.00	0.00

with respect to the structure of the model and its performance. Events such as the simultaneous transport and assimilation of nitrate and ammonium (Zevenboom & Mur 1981; Quegumer *et al.* 1986; Zehr *et al.* 1989) may be readily accounted for. Although not an aim of the model, the simulation of the responses of the GLN pool to N starvation and refeeding with nitrate or ammonium is realistic on a quantitative and temporal basis (e.g. Wood & Flynn 1995). However, in reality, GLN rarely sinks to essentially zero concentration. The behaviour of the model in predicting growth using ammonium or nitrate at different levels of light are also in keeping with reports in the literature (Thompson *et al.* 1989; Wood & Flynn 1995). Thus any difference in growth rates is most apparent at high PFDs (figure 10, satisfying table 1(xii)).

A prediction of the model is that, in addition to the expected depression of nitrate transport in the presence of ammonium (figure 11*b*), nitrate may also depress the transport of ammonium (figure 11*a*). The existence of such an event has been suggested by the results of Caperon & Zieman (1976), Terry (1982) and Dortch & Conway (1984). In the model this event occurs when the supply of external ammonium is limiting and hence GLN levels are not high enough to affect the use of nitrate. The addition of nitrate results in the formation of internal ammonium and GLN which affects the uptake of both nitrate and

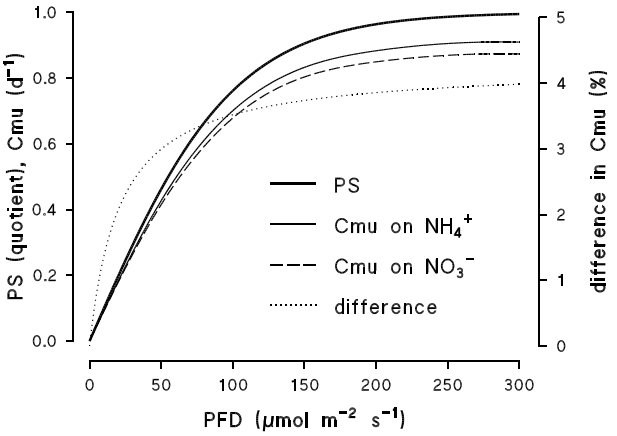

Figure 10. Comparison of steady-state C-specific growth rates (Cmu), using either 1.4 μg N ml^{-1} (100 μM) ammonium or nitrate at different photon flux densities. The model was as defined in tables 2–7, except that Kq was doubled to emphasis the difference in growth rates. The value of PS was computed as PS = tanh($\alpha \cdot$ PFD), where α was set at 0.01. The difference in growth rates is consistent with table 1(xii).

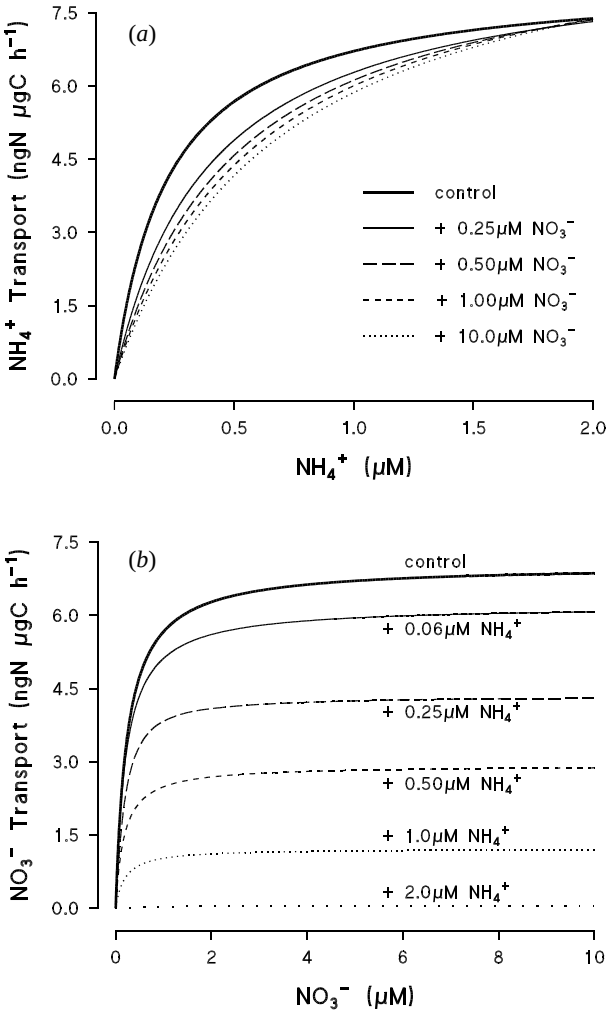

Figure 11. Effects of external nitrate concentration on ammonium transport (*a*); and external ammonium concentration on nitrate transport (*b*) under steady-state conditions.

ammonium. However, increasing the concentration of nitrate does not result in a further depression of ammonium transport because the GLN produced by the assimilation of both N sources affects the transport of nitrate more than ammonium.

All these aspects of the behaviour of the model support our contention that it offers a reasonable basis for simulating generalized phytoplankton behaviour with respect to ammonium–nitrate interactions. The normalization of various components to *Umax* and to the size of internal nutrient pools facilitates the simulation of phytoplankton of different physiological character. Cell size is not a specified parameter, but cells of different size may have different transport characteristics (Aksnes & Egge 1991), grow at different rates and have nutrient pools of different sizes. These facets may be readily changed within the model enabling an exploration of size-related ammonium–nitrate interactions (Probyn 1985; Stolte *et al.* 1994).

The aim to produce a comprehensive model for simulating interactions between ammonium and nitrate creates an immediate conflict between the desires of the modeller, who wishes to keep things as simple as possible, and the physiologist, who will wish to include every subtlety in an attempt to mimic reality. Davidson & Cunningham (1996) argue against the inclusion of internal nutrient pools in algal models because of problems of parametrization. However, we would suggest that the inclusion of such pools is essential if an adequate simulation of ammonium–nitrate interactions is required. At present, all the relevant biochemical processes are difficult to parametrize adequately and our knowledge of the form of such regulations is minimal. The omission of various components of the current model in an attempt to simplify the system, or the use of RH rather than sigmoidal functions in regulatory steps resulted in a failure to reproduce all of the salient features of the interaction demonstrated in the present model.

The use of C as a base for the model has serious implications for parametrization. Most studies of algal N metabolism do not include measurements of C (or biovolume with which it closely correlates (Montagnes *et al.* 1994)), but express N uptake in units of cell number, N, protein or chlorophyll. As a result, the N status of the cells (as indicated by the N:C ratio) is often unknown. In many studies, the N status of the cell has been related to a period of N deprivation, or to growth rate in steady state conditions rather than to the N:C ratio. Although many data may be of use on a qualitative basis, they may be of little use on a quantitative basis, and comparisons between different data sets are complicated.

An assumption made for the derivation of Tq values (figure 5) has been that nitrate-grown cells subjected to N deprivation are physiologically similar to N deprived ammonium-grown cells. Given that the lipid content of cells growing on these N sources may be very different (Flynn *et al.* 1992) it is possible that by the time growth stops (i.e. Q = Qo) the cells are

PHILOSOPHICAL TRANSACTIONS OF THE ROYAL SOCIETY B BIOLOGICAL SCIENCES

still dissimilar and will thus respond differently when re-fed with nitrate or ammonium. The calculation of Tq could be simulated using synthesis and decay (protein turnover) processes similar to that used for NNiR, perhaps with an induction of nitrate transporters (Miyagi *et al.* 1992). There is little experimental evidence to indicate the relative importance of alternative strategies, but it would be simple to incorporate such subtlety within the current model structure.

While the rate processes of uptake at the whole cell level have been measured, and the qualitative nature of intracellular processes studied, the *quantitative* nature of interactions at the intracellular level are largely unknown. Most of our knowledge of the enzymatic reduction of nitrate has resulted from *in vitro* studies (e.g. Everest *et al.* 1986) and few of these have been performed on phytoplankton of ecological importance. Enzyme assays are usually conducted under conditions of non-limiting substrate concentrations, although they may be limiting *in vivo*. Berges & Harrison (1995) suggest the use of *in vitro NR* assays to estimate nitrate assimilation. For the simulation in continuous light (figure 7) NNiR correlates reasonably well with nitrate transport and with NO3red (simulating *in vivo NR* activity), but the correlation becomes poor as nitrate becomes exhausted (figure 12*a*) and is especially poor in a simulation of growth in a L:D cycle (figures 8, 12*b*). It has also been suggested that cells may retain a low constitutive level of NR (Herrera *et al.* 1972; Rigano 1973). Because the size of the nitrite pool appears to be very small, and thus the ratio of (pool size:flow through pool) becomes smaller, adequate regulation in a model including such a step is critical. However, our knowledge of the regulation of NiR in phytoplankton is very limited, hence the omission of a specific nitrite pool and NiR activity in the present model. As a consequence, the model cannot yet simulate the excretion of nitrite reported under certain conditions (e.g. Sciandra & Amara 1994).

The identity of the organic regulator (or regulators) of inorganic N assimilation is not known but we have assumed that it is GLN or a compound biochemically very close to it. GLN is the product of two GS enzymes which reside in different compartments in the cell (e.g. Ahmed & Hellebust 1988). Pool sizes have been estimated from whole-cell extracts, so we know little or nothing about the compartmentalization of GLN (or of ammonium and nitrate) during different phases of the nutrient history of eukaryote algae. Both the synthesis of GLN and the subsequent use of GLN for other processes require C skeletons. In this respect, algae appear to fall into two groups: those in which GLN rises (or at least does not fall significantly) in the dark; and those in which GLN falls rapidly (Flynn 1990*b*; Flynn *et al.* 1993). Depending on the values of CGOGAT and CAAs, either of these possibilities can be simulated (not shown). For the operation of the model, given that GLN is being used to regulate nutrient transport, NNiR synthesis, as well as GS activity, this difference in metabolism can have profound effects.

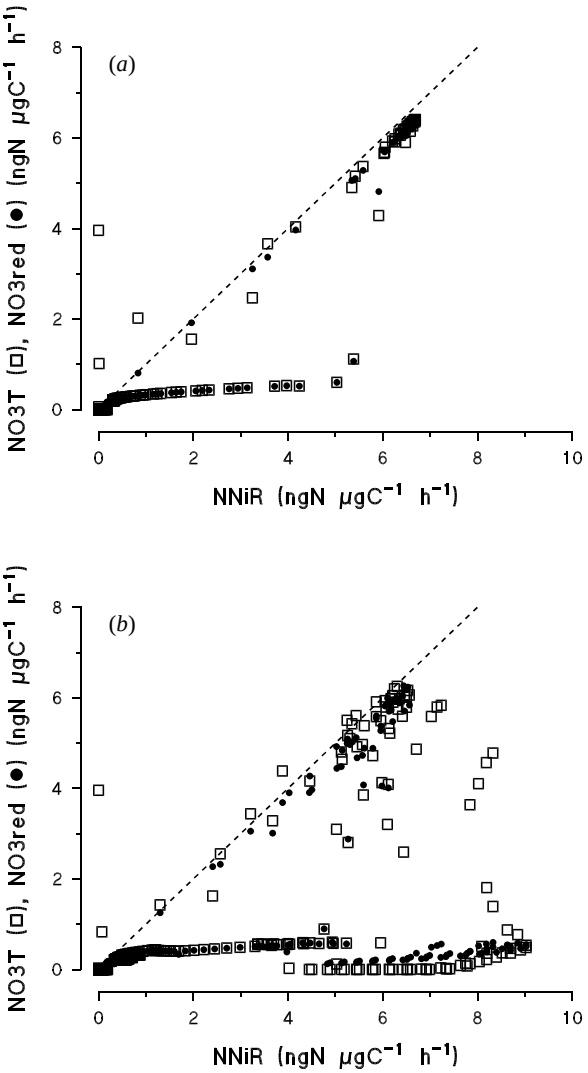

Figure 12. Relationships between the maximum enzyme activity for the reduction of nitrate to ammonium (NNiR, analogous to *in vitro* enzyme assay), the actual rate of reduction of nitrate to ammonium (NO3red) and nitrate transport (NO3T). Data are taken from the simulations shown for continuous light in figure 7*a* and in a light–dark cycle in figure 8*b*. The dashed line indicates the 1:1 ratio between transport and enzyme activity.

The absence of information about transport and assimilation in the dark by algae of different nutrient status is a particular problem, particularly since most laboratory studies make use of continuous illumination and/or steady-state conditions (e.g. Bienfang 1975; Caperon & Zieman 1976; Berges & Harrison 1995), thus simplifying experiment design and interpretation (see figures 7, 8). In nature, on average, perhaps half the organism's time may be spent in darkness, resulting in the initiation of diel cycles (Eppley *et al.* 1971; Goldman & Dennett 1983; Cullimore & Sims 1981*b*) which may have a particular significant effect on the use of oxidized N (Grant & Turner 1969), as indicated by the model (figures 8, 9). The ability to assimilate N in the dark is also species specific (Paasche *et al.* 1984; Rainbault & Mingazzini 1987), as is the ability to use alternative N sources such as nitrite, urea and dissolved free amino acids (McCarthy 1981; Wheeler 1983; Flynn 1990*a*).

PHILOSOPHICAL TRANSACTIONS OF THE ROYAL SOCIETY B BIOLOGICAL SCIENCES

The model simulates a hypothetical species. Every species and major taxonomic group will differ with respect to many facets of their behaviour. However, the fact that the model appears robust and can satisfactorily simulate the expected behaviour of marine phytoplankton in general suggests that it can be used to generate hypotheses for testing experimentally. This may ease the enormous task of testing factorial permutations of nutrient status, substrate concentrations, growth rates, light interactions, nutrient pool sizes, etc., which are a serious impediment to designing experiments which may then take many months or years to conduct. Arguably, after four decades of detailed study, the subject needs the development of a unifying basis to direct future work. Weaknesses in the model due to inadequate experimental evidence may also be considered as directors for future studies.

This work was funded by the Natural Environment Research Council of the UK. The authors wish to thank Nick Owens (University of Newcastle, UK) and Roel Riegman and Willem Stolte (Netherlands Institute for Sea Research) for their contributions to discussions during the development of this model.

REFERENCES

Ahmed, I. & Hellebust, J. A. 1988 Enzymology of ammonium assimilation in three green flagellates. *New Phytol.* **109**, 415–421.

Akimova, N. I., Evstigneeva, Z. G. & Kretovich, V. L. 1976 Regulation of glutamine metabolism in *Chlorella pyrenoidosa*. Regulation of glutamine synthetase activity in *Chlorella* by amino acids. *Biokhimiya* **41**, 1471–1477.

Aksnes, D. L. & Egge, J. K. 1991 A theoretical model for nutrient uptake in phytoplankton. *Mar. Ecol. Prog. Ser.* **70**, 65–72.

Beardall, J. & Raven, J. A. 1990 Pathways and mechanisms of respiration in microalgae. *Mar. Microb. Food Webs* **4**, 7–30.

Berges, J. A. & Harrison, P. J. 1995 Nitrate reductase activity quantitatively predicts the rate of nitrate incorporation under steady state light limitation: a revised assay and characterisation of the enzyme in three species of marine phytoplankton. *Limnol. Oceanogr.* **40**, 82–93.

Bienfang, P. K. 1975 Steady-state analysis of nitrate–ammonium assimilation by phytoplankton. *Limnol. Oceanogr.* **20**, 402–411.

Blasco, D. & Conway, H. L. 1982 Effect of ammonium on the regulation of nitrate assimilation in natural phytoplankton populations. *J. Exp. Mar. Biol. Ecol.* **61**, 157–168.

Campbell, W. H. 1996 Nitrate reductase biochemistry comes of age. *Plant Physiol.* **111**, 355–361.

Caperon, J. 1968*a* Population growth in micro-organisms limited by food supply. *Ecology* **49**, 715–721.

Caperon, J. 1968*b* Population growth responses of *Isochrysis galbana* to nitrate variation at limiting concentrations. *Ecology* **49**, 866–872.

Caperon, J. & Ziemann, D. A. 1976 Synergistic effects of nitrate and ammonium ion on the growth and uptake kinetics of *Monochrysis lutheri* in continuous culture. *Mar. Biol.* **36**, 73–84.

Clayton, J. R. & Ahmed, S. I. 1987 Modified assay procedure for enhanced sensitivity of *in vitro* glutamine synthetase (GS) activity measurements in marine phytoplankton. *Mar. Ecol. Prog. Ser.* **36**, 177–180.

Collos, Y. 1982 Transient situations in nitrate assimilation by marine diatoms. 3. Short term uncoupling of nitrate uptake and reduction. *J. Exp. Mar. Biol. Ecol.* **62**, 285–295.

Collos, Y. 1983 Transient situations in nitrate assimilation by marine diatoms. 4. Non-linear phenomena and the estimation of the maximum uptake rate. *J. Plankton Res.* **5**, 677–691.

Collos, Y. 1989 A linear model of external interactions during uptake of different forms of inorganic nitrogen by microalgae. *J. Plankton Res.* **11**, 521–533.

Conway, H. L. 1977 Interactions of inorganic nitrogen in the uptake and assimilation by marine phytoplankton. *Mar. Biol.* **39**, 221–232.

Cresswell, R. C. & Syrett, P. J. 1979 Ammonium inhibition of nitrate uptake by the diatom *Phaeodactylum tricornutum*. *Plant Sci. Lett.* **14**, 321–325.

Cullen, J. J. & Horrigan, S. G. 1981 Effects of nitrate on the diurnal vertical migration, carbon to nitrogen ratio, and the photosynthetic capacity of the dinoflagellate *Gymnodinium splendens*. *Mar. Biol.* **62**, 81–89.

Cullimore, J. V. & Sims, A. P. 1981*a* Glutamine-synthetase of *Chlamydomonas*—its role in the control of nitrate assimilation. *Planta* **153**, 18–24

Cullimore, J. V. & Sims, A. P. 1981*b* Pathways of ammonia assimilation in illuminated and darkened *Chlamydomonas reinhardii*. *Phytochemistry* **20**, 933–940.

Davidson, K. & Cunningham, A. 1996 Accounting for nutrient processing time in mathematical models of phytoplankton growth. *Limnol. Oceanogr.* **41**, 779–783.

Demanche, J. M., Curl Jr, H. C., Lundy, D. W. & Donaghay, P. L. 1979 The rapid response of the marine diatom *Skeletonema costatum* to changes in external and internal nutrient concentration. *Mar. Biol.* **53**, 323–333.

Dixon, G. K. & Syrett, P. J. 1988 Interactions between the uptake and assimilations of inorganic nitrogen and carbon in *Amphidinium* spp. (Dinophyceae). *J. Exp. Bot.* **39**, 1299–1311.

Dortch, Q. 1982 Effect of growth conditions on accumulation of internal nitrate, ammonium, amino acids and protein in three marine diatoms. *J. Exp. Mar. Biol. Ecol.* **61**, 243–264.

Dortch, Q. 1990 The interaction between nitrate and ammonium uptake in phytoplankton. *Mar. Ecol. Prog. Ser.* **61**, 183–201.

Dortch, Q. & Conway, H. L. 1984 Interaction between nitrate and ammonium uptake; variation with growth rate, nitrogen source, and species. *Mar. Biol.* **79**, 151–164.

Dortch, Q., Clayton, J. R., Thoresen, S. S., Bressler, S. L. & Ahmed, S. I. 1982 Response of marine phytoplankton to nitrogen deficiency: decreased nitrate uptake vs enhanced ammonium uptake. *Mar. Biol.* **70**, 13–19.

Dortch, Q., Clayton, J. R., Thoresen, S. S. & Ahmed, S. I. 1984 Species differences in accumulation of nitrogen pools in phytoplankton. *Mar. Biol.* **81**, 237–250.

Droop, M. R. 1968 Vitamin B_{12} and marine ecology IV. The kinetics of uptake, growth and inhibition in *Monochrysis lutheri*. *J. Mar. Biol. Ass. UK* **48**, 689–733.

Dugdale, R. C. & Goering, J. J. 1967 Uptake of new and regenerated forms of nitrogen in primary production. *Limnol. Oceanogr.* **12**, 196–206

Eppley, R. W., Coatsworth, J. L. & Solorzano, L. 1969*a*

Studies of nitrate reductase in marine phytoplankton. *Limnol. Oceanogr.* **14**, 194–205.

Eppley, R. W., Rogers, J. N. & McCarthy, J. J. 1969*b* Half-saturation constants for uptake of nitrate and ammonium by marine phytoplankton. *Limnol. Oceanogr.* **14**, 912–919.

Eppley, R. W., Rogers, J. N., McCarthy, J. J. & Sournia, A. 1971 Light/dark periodicity in nitrogen assimilation of the marine phytoplankters *Skeletonema costatum* and *Coccolithus huxleyi* in N-limited chemostat culture. *J. Phycol.* **7**, 150–154.

Everest, S. A., Hipkin, C. R. & Syrett, P. J. 1986 Enzyme activities in some marine phytoplankters and the effect of nitrogen limitation on nitrogen and carbon metabolism in *Chlorella stigmatophora*. *Mar. Biol.* **90**, 165–172.

Fasham, M. J. R. 1993 Modelling the marine biota. In *The global carbon cycle* (ed. M. Heiman), pp. 457–504. NATO ASI Ser. I15. Springer.

Faure, J. D., Vincentz, M., Kronenberger, J. & Caboche, M. 1991 Co-regulated expression of nitrate and nitrite reductases. *FEBS Lett.* **392**, 1–5.

Flynn, K. J. 1990*a* Composition of intracellular and extracellular pools of amino acids, and amino acid utilization of microalgae of different sizes. *J. Exp. Mar. Biol. Ecol.* **139**, 151–166.

Flynn, K. J. 1990*b* The determination of nitrogen status in microalgae. *Mar. Ecol. Prog. Ser.* **61**, 297–307.

Flynn, K. J. 1991 Algal carbon-nitrogen metabolism: a biochemical basis for modelling the interactions between nitrate and ammonium uptake. *J. Plankton Res.* **13**, 373–387.

Flynn, K. J., Dickson, D. M. J. & Al-Amoudi, O. A. 1989 The ratio of glutamine: glutamate in microalgae: a biomarker for N-status suitable for use at natural cell densities. *J. Plankton Res.* **11**, 165–170.

Flynn, K. J., Garrido, J. L., Zapata, M., Opik, H. & Hipkin, C. R. 1992 Changes in fatty acids, amino acids and carbon/nitrogen biomass during nitrogen starvation of ammonium and nitrate grown *Isochrysis galbana*. *J. Appl. Phycol.* **4**, 95–104.

Flynn, K., Flynn, K. J. & Jones, K. J. 1993 Changes in dinoflagellate intracellular amino acids in response to diurnal changes in light and N-supply. *Mar. Ecol. Prog. Ser.* **100**, 245–252

Flynn, K., Jones, K. J. & Flynn, K. J. 1996 Comparisons among species of *Alexandrium* (Dinophyceae) grown in nitrogen or phosphorus-limiting batch culture. *Mar. Biol.* **126**, 9–18.

Geider, R. J., MacIntyre, H. L. & Kana, T. M. 1996 A dynamic model of photoadaptation in phytoplankton. *Limnol. Oceanogr.* **41**, 1–15

Glibert, P. M. & McCarthy, J. J. 1984 Uptake and assimilation of ammonium and nitrate by phytoplankton. Indices of nutritional status for natural assemblages. *J. Plankton Res.* **6**, 667–697.

Goldman, J. C. & Dennett, M. R. 1983 Effect of nitrogen sources on short term light and dark CO_2 uptake by a marine diatom. *Mar. Biol.* **76**, 7–15.

Grant, B. R. & Turner, I. M. 1969 Light-stimulated nitrate and nitrite assimilation in several species of algae. *Comp. Biochem. Physiol.* **29**, 995–1004.

Haefner J. W. 1996 *Modeling biological systems*. New York: Chapman and Hall.

Harrison, W. G., Harris, L. R. & Irwin, B. D. 1996 The kinetics of nitrogen utilization in the oceanic mixed layer: Nitrate and ammonium interactions at nanomolar concentrations. *Limnol. Oceanogr.* **41**, 16–32

Harrison, W. G., Platt, T. & Irwin, B. 1982 F-ratio and its relationship to ambient nitrate concentration in coastal waters. *J. Plankton Res.* **9**, 235–248.

Herrera, J., Panequé, A., Maldonado, J., Barea, J. L. & Losada, M. 1972 Regulation by ammonium of nitrate reductase synthesis and activity in *Chlamydomonas reinhardi*. *Biochem. Biophys. Res. Comm.* **48**, 996–1003

Hipkin, C. R. 1989 Nitrate assimilation in yeasts. In *Molecular and genetic aspects of nitrate assimilation* (ed. J. L. Wray & J. R. Kinghorn), pp. 51-68. Oxford: Oxford Science Publications.

Hipkin, C. R. & Syrett, P. J. 1977 Some effects of nitrogen-starvation on nitrogen and carbohydrate metabolism in *Ankistrodesmus braunii*. *Planta* **133**, 209–214.

Hipkin, C. R., Thomas, R. T. & Syrett, P. J. 1983 Effects of nitrogen deficiency on nitrate reductase, nitrate assimilation and photosynthesis in unicellular marine algae. *Mar. Biol.* **77**, 101–105.

Horrigan, S. G. & McCarthy, J. J. 1982 Phytoplankton uptake of ammonium and urea during growth on oxidised forms of nitrogen. *J. Plankton Res.* **4**, 379–389.

Jassby, A. D. & Platt, T. 1976 Mathematical formulation of the relationship between photosynthesis and light for phytoplankton. *Limnol. Oceanogr.* **21**, 540–547.

Levasseur, M., Thompson, P. A. & Harrison, P. J. 1993. Physiological acclimation of marine phytoplankton to different nitrogen sources. *J. Phycol.* **29**, 587–595.

Laws, E. A. & Caperon, J. 1976 Carbon and nitrogen metabolism by *Monochrysis lutheri*: measurement of growth rate dependent respiration rates. *Mar. Biol.* **36**, 85–97.

Losada, M. 1980 The photosynthetic assimilation of nitrate. In *Conf. Proc. II Congress of Federation of European Soc. of Plant Physiology, Santiago, Sociedad Española de Fisiologia Vegetal*, pp. 112–113. Santiago.

Lund, B. A. 1987 Mutual interference of ammonium, nitrate and urea on uptake of ^{15}N sources by the marine diatom *Skeletonema costatum*. *J. Exp. Mar. Biol. Ecol.* **113**, 167–180.

McCarthy, J. J. 1981 The kinetics of nutrient utilization. *Can. Bull. Fish. Aquat. Sci.* **210**, 211–233.

McCarthy, J. J., Taylor, W. R. & Taft, J. L. 1975 The dynamics of nitrogen and phosphorous cycling in the open waters of Chesapeake Bay. In *Marine chemistry in the coastal environment* (ed. T. M. Church) ACS Symp. Ser. 18, pp. 664–681.

Maestrini, S. Y., Robert, J. M., Leftley, J. W. & Collos, Y. 1986 Ammonium thresholds for simultaneous uptake of ammonium and nitrate by oyster-pond algae. *J. Exp. Mar. Biol. Ecol.* **102**, 75–98.

Miflin, B. J. & Lee, P. J. 1980 Ammonia assimilation. In *The biochemistry of plants 5* (ed. B. J. Miflin), pp. 169–202. Academic.

Montagne, D. J. S, Berges, J. A., Harrison, P. J. & Taylor, F. J. R. 1994 Estimating carbon, nitrogen, protein and chlorophyll a from volume in marine phytoplankton. *Limnol. Oceanogr.* **39**, 1044–1060.

Miyagi, N., Satoh, S. & Fuji, T. 1992 A nitrate-inducible plasma membrane protein of a marine alga, *Heterosigma akashiwo*. *Plant Cell Physiol.* **33**, 971–976.

Osborne, B. A. & Geider, R. J. 1986 Effect of nitrate–nitrogen limitation on photosynthesis of the diatom *Phaeodactylum tricornutum* Bohlin (Bacillariophyceae). *Plant Cell Environ.* **9**, 617–625.

Paasche, E., Bryceson, I. & Tangen, K. 1984 Interspecific variation in dark nitrogen uptake by dinoflagellates. *J. Phycol.* **20**, 394–401.

Parker, R. A. 1993 Dynamic models for ammonium inhi-

PHILOSOPHICAL TRANSACTIONS OF THE ROYAL SOCIETY B BIOLOGICAL SCIENCES

bition of nitrate uptake by phytoplankton. *Ecol. Modelling.* **66**, 113–120.
Probyn, T. A. 1985 Nitrogen uptake by size-fractionated phytoplankton populations in the southern Benguela upwelling system. *Mar. Ecol. Prog. Ser.* **22**, 249–258.
Quegumer, B., Hafsour, M. & Treguer, P. 1986 Simultaneous uptake of ammonium and nitrate by phytoplankton in coastal ecosystems. *Estuar. Coast. Shelf Sci.* **23**, 751–757.
Rainbault, P. & Mingazzini, M. 1987 Diurnal variations of intracellular nitrate storage by marine diatoms: effects of nutritional state. *J. Exp. Mar. Biol. Ecol.* **112**, 217–232.
Raven, J. A. 1980 Nutrient transport in microalgae. *Adv. Microbiol. Physiol.* **21**, 47–226.
Rigano, C. 1973 Effect of nitrate, ammonia and nitrogen starvation on the regulation of nitrate reductase in *Cyanidium caldarium*. *Arch. Microbiol.* **90**, 27–33.
Rigano, C., Rigano, V. D. M., Vona, V. & Fuggi, A. 1979 Glutamine synthetase activity, ammonia assimilation and control of nitrate reduction in the unicellular red alga *Cyanidium caldarium*. *Arch. Microbiol.* **121**, 117–120.
Roberston, D. L. & Alberte, R. S. 1996 Isolation and characterization of glutamine synthetase from the marine diatom *Skeletonema costatum*. *Plant Physiol.* **111**, 1169–1175.
Schnell, R. A. & Lefebvre, P. A. 1993 Isolation of the *Chlamydomonas* regulatory gene *NIT*2 by transposon tagging. *Genetics* **134**, 737–747.
Sciandra, A. & Amara, R. 1994 Effects of nitrogen limitation on growth and nitrite excretion rates of the dinoflagellate *Prorocentrum minimum*. *Mar. Ecol. Prog. Ser.* **105**, 301–309.
Serra, J. L., Llama, M. J. & Codenas, E. 1978 Nitrate utilization by the diatom *Skeletonema costatum*. 2. Regulation of nitrate uptake. *Plant Physiol.* **62**, 991–994.
Sherman, T. P., Erwin, M. A. & Funkhouser, E. A. 1983 Changes in nitrate reductase protein during loss and gain of nitrate reductase activity in *Chlorella vulgaris*. *Biochim. Biophys. Acta.* **749**, 265–269.
Solomonson, L. P. & Barber, M. J. 1990 Assimilatory nitrate reductase: functional properties and regulation. *A. Rev. Plant Physiol. Plant Molec. Biol.* **41**, 225–253.
Solomonson, L. P. & Spehar, A. M. 1977 Model for the regulation of nitrate assimilation. *Nature* **265**, 373–375.
Stolte, W. & Riegman, R. 1996 A model approach for size selective competition of marine phytoplankton for fluctuating nitrate and ammonium. *J. Phycol.* **32**, 732–740.
Stolte, W., McCollin, T., Noordeloos, A. A. M. & Riegman, R. 1994 Effect of nitrogen source on the size distribution within marine phytoplankton populations. *J. Exp. Mar. Biol. Ecol.* **184**, 83–97.
Syrett, P. J. 1956*a* The assimilation of ammonia and nitrate by nitrogen starved cells of *Chlorella vulgaris*. II The assimilation of large quantities of nitrogen. *Physiol. Plant* **9**, 19–27.
Syrett, P. J. 1956*b* The assimilation of ammonia and nitrate by nitrogen starved cells of *Chlorella vulgaris*. III Differences of metabolism dependent on the nature of the nitrogen source. *Physiol. Plant* **9**, 28–37.
Syrett, P. J. 1981 Nitrogen metabolism of microalgae. *Can. Bull Fish. Aquat. Sci.* **210**, 182–210.
Syrett, P. J. & Hipkin, C. R. 1973 The appearance of nitrate reductase activity in nitrogen-starved cells of *Ankistrodesmus braunii*. *Planta* **111**, 57–64.
Syrett, P. J. & Morris, I. 1963 The inhibition of nitrate assimilation by ammonium in *Chlorella*. *Biochim. Biophys. Acta* **67**, 566–575.
Syrett, P. J. & Peplinska, A. M. 1988 Effects of nitrogen-deprivation, and recovery from it, on the metabolism of microalgae. *New Phytol.* **109**, 289–296.
Syrett, P. J., Flynn, K. J., Molloy, C. J., Dixon, G. K., Peplinska, A. M. & Cresswell, R. C. 1986 Effects of nitrogen deprivation on rates of uptake of nitrogenous compounds by the marine diatom *Phaeodactylum tricornutum* Bohlin. *New Phytol.* **102**, 39–44.
Terry, K. L. 1982 Nitrate uptake and assimilation in *Thalassiosira weissflogii* and *Phaeodactylum tricornutum*; interactions with photosynthesis and with uptake of other ions. *Mar. Biol.* **69**, 21–30.
Thompson, P. A., Levessaur, M. E. & Harrison, P. J. 1989 Light-limited growth on ammonium vs nitrate: what is the advantage for marine phytoplankton? *Limnol. Oceanogr.* **34**, 1014–1024.
Turpin, D. H. 1991 Effects of inorganic N availability on algal photosynthesis and carbon metabolism. *J. Phycol.* **27**, 14–20.
Turpin, D. H., Elriffi, I. R., Birk, D. G., Wegner, H. G. & Holmes, J. J. 1988 Interactions between photosynthesis, respiration and nitrogen assimilation in microalgae. *Can. J. Bot.* **66**, 2083–2097.
Valasco, P. J., Tischner, R., Huffaker, R. C. & Whitaker, J. R. 1988 Synthesis and degradation of nitrate reductase during the cell cycle of *Chlorella sorokiniana*. *Plant Physiol.* **89**, 220–224.
Watanabe, M. M., Nakamura, Y., Mori, S. & Yamochi, S. 1982 Effects of physiochemical factors and nutrients on the growth of *Heterosigma akashiwo* Hada from Osaka Bay, Japan. *Jap. J. Phycol. (Sorui)* **30**, 279–288.
Wheeler, P. A. 1983 Phytoplankton nitrogen metabolism. In *Nitrogen in the marine environment* (ed. E. J. Carpenter & D. G. Capone), pp. 309–346. Academic.
Wood, G. & Flynn, K. J. 1995 Growth of *Heterosigma carterae* (Raphidophyceae) on nitrate and ammonium at three photon flux densities: Evidence for N-stress in nitrate-growing cells. *J. Phycol.* **31**, 859–867
Wray, J. L. 1989 Molecular and genetic aspects of nitrite reductase in higher plants. In *Molecular and genetic aspects of nitrate assimilation* (ed. J. L.Wray & J. R. Kinghorn), pp. 244–262. Oxford: Oxford Science Publications.
Zehr, J. P., Capone, D. G. & Falkowski, P. G. 1989 Rapid incorporation of $^{13}NO_3$ by NH_4-limited phytoplankton. *Mar. Ecol. Prog. Ser.* **51**, 237–241.
Zevenboom, W. & Mur, L. R. 1981 Simultaneous short term uptake of nitrate and ammonium by *Oscillatoria agardhii* grown in nitrate or light-limited continuous culture. *J. Gen. Microbiol.* **126**, 355–363.

Received 4 November 1996; accepted 6 January 1997

PHILOSOPHICAL TRANSACTIONS OF THE ROYAL SOCIETY B BIOLOGICAL SCIENCES

PHILOSOPHICAL TRANSACTIONS OF THE ROYAL SOCIETY B BIOLOGICAL SCIENCES